Biosci. Rep. (2013) / **33** / art:e00007 / doi 10.1042/BSR20120031

Supplementary data

Original Paper

OPEN ACCESS

Bioscience Reports

www.bioscirep.org

Acute regulation of 5′-AMP-activated protein kinase by long-chain fatty acid, glucose and insulin in rat primary adipocytes

Abdel HEBBACHI and David SAGGERSON[1]

Institute of Structural and Molecular Biology, Division of Biosciences, University College London, Gower Street, London WC1E 6BT, U.K.

Synopsis

Palmitate increased AMPK (5′-AMP-activated protein kinase) activity, glucose utilization and 2-DOG (2-deoxyglucose) transport in rat adipocytes. All three effects were blocked by the AMPK inhibitor Compound C, leading to the conclusion that in response to an increase in long-chain NEFA (non-esterified fatty acid) concentration AMPK mediated an enhancement of adipocyte glucose transport, thereby providing increased glycerol 3-phosphate for FA (fatty acid) esterification to TAG (triacylglycerol). Activation of AMPK in response to palmitate was not due to an increase in the adipocyte AMP:ATP ratio. Glucose decreased AMPK activity and effects of palmitate and glucose on AMPK activity were antagonistic. While insulin had no effect on basal AMPK activity insulin did decrease AMPK activity in the presence of palmitate and also decreased the percentage effectiveness of palmitate to increase the transport of 2-DOG. It is suggested that activation of adipocyte AMPK by NEFA, as well as decreasing the activity of hormone-sensitive lipase, could modulate adipose tissue dynamics by increasing FA esterification and, under certain circumstances, FA synthesis.

Key words: acute regulation, adipocyte, AMP kinase, fatty acid, glucose, insulin

Cite this article as: Hebbachi, A. and Saggerson, D. (2013) Acute regulation of 5′-AMP-activated protein kinase by long-chain fatty acid, glucose and insulin in rat primary adipocytes. Biosci. Rep. **33**(1), art:e00007.doi:10.1042/BSR20120031

INTRODUCTION

White adipocytes are important in mammalian energy homoeostasis since they store TAG (triacylglycerol), the body's main energy reserve. The long-chain NEFA (non-esterified fatty acid) precursors of adipocyte TAG are (i) derived from plasma lipoproteins, (ii) arise by *de novo* synthesis within adipocytes or (iii) are provided for re-esterification secondary to lipolysis. The other essential TAG precursor is glycerol 3-phosphate. Adipocytes have minimal expression of glycerol kinase and normally glyceroneogenesis from 3-carbon precursors is low [1]. Therefore cellular glycerol 3-phosphate is largely derived from plasma glucose whose entry into adipocytes is mainly facilitated by the insulin-activated glucose transporter GLUT4. Diagrams that describe in more detail the 'glucose economy' and the 'FA (fatty acid) economy' of adipocytes are shown in Supplementary Figures S1 and S2 (at http://www.bioscirep.org/bsr/033/bsr033e007add.htm).

The effect of insulin to stimulate glucose transport in skeletal or cardiac muscle cells and in adipocytes through increasing the abundance of GLUT4 at the cell surface is well known. Additionally, in skeletal muscle [2] and in cardiac myocytes [3] GLUT4 translocation and glucose transport are increased following activation of the AMPK (5′-AMP-activated protein kinase). The AMPK is a heterotrimeric ($\alpha\beta\gamma$) serine/threonine protein kinase that is a key regulator of energy homoeostasis. AMPK is allosterically activated by an increase in the cellular AMP:ATP ratio which also promotes covalent activation of AMPK (at α-Thr^{172} in the activation loop of the catalytic subunit) by upstream AMPKs because binding of AMP to the kinase γ-subunit renders the α-Thr^{172} phosphorylation site a poorer substrate for protein phosphatases. Therefore AMPK is activated during cellular energy stress. Previously it has been realized that several neuroendocrine factors, including insulin, regulate AMPK phosphorylation/activity in tissue-specific ways [4,5] that are mainly independent of energy stress and changes in the AMP:ATP ratio. Also the AMPK system can register the availabilities of carbohydrate and lipid metabolic fuels under conditions where the AMP:ATP ratio is unchanged. Palmitate increases AMPK α-Thr^{172} phosphorylation and activity with

Abbreviations used: ACC, acetyl-CoA carboxylase; AICAR, 5-amino-4-imidazolecarboxamide-1-β-D-ribofuranoside; AMPK, 5′-AMP-activated protein kinase; 2-DOG, 2-deoxyglucose; FA, fatty acid; GLUT4, glucose transporter 4; LPL, lipoprotein lipase; NEFA, non-esterified fatty acid; PDH, pyruvate dehydrogenase; PI3K, phosphoinositide 3-kinase; TAG, triacylglycerol.

[1] To whom correspondence should be addressed (email d.saggerson@ucl.ac.uk).

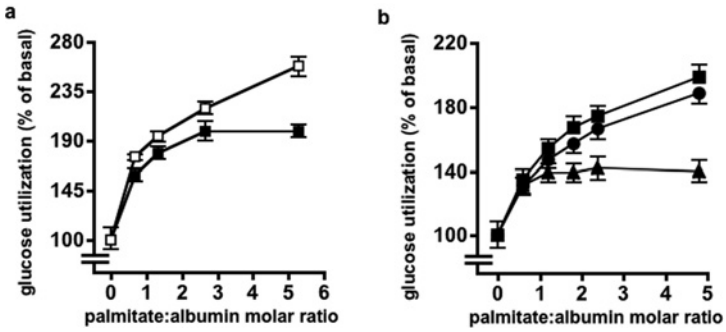

Figure 1 Palmitate increased calculated rates of glucose utilization by adipocytes

Values for FA, GG, lactate and pyruvate were taken from Table 3 of [22] (**a**) and from Table 9 and Figure 3 of [22] (**b**). Adipocytes ($n = 5$ in all cases) were incubated for 1 h with 5% (w/v) BSA (**a**) or 2.75% (w/v) BSA (**b**) together with sodium palmitate. Abscissa values are expressed as palmitate:albumin molar ratios in order to allow comparison between these two experiments. Eqn (1.8) in the Supplementary Online data section (at http://www.bioscirep.org/bsr/033/bsr033e007add.htm) was used to calculate glucose utilization. (**a**) Adipocytes were from fed rats. Basal rates of glucose utilization with 5 mM glucose + 0.2 μM insulin (filled symbols) were 10.4 ± 0.8 μmol $\cdot$ h^{-1} $\cdot$ 100 μg of DNA^{-1} and with 1 mM glucose (open symbols) were 2.6 ± 0.3 μmol $\cdot$ h^{-1} $\cdot$ 100 μg of DNA^{-1}. (**b**) Basal rates of glucose utilization with 5 mM glucose + 0.2 μM insulin were 8.9 ± 0.7, 6.7 ± 0.5 and 5.4 ± 0.4 μmol $\cdot$ h^{-1} $\cdot$ 100 μg of DNA^{-1} for cells from fed (squares), 24 h-starved (circles) and 72 h-starved (triangles) rats. All tested additions of palmitate increased glucose utilization to at least the $P < 0.005$ significance level.

subsequent phosphorylation of ACC (acetyl-CoA carboxylase) in heart [6] and in L6 skeletal muscle myotubes [7,8] – an effect that is also seen with other long-chain NEFAs, e.g. oleate [6] and linoleate [8]. By contrast AMPK α-Thr^{172} phosphorylation and activity as well as ACC phosphorylation are decreased by glucose in skeletal muscle [9] and cardiac myocytes [10]. In 2005, Daval et al. [11] noted 'whereas the function of AMPK in liver and muscle has been well illustrated, its role in adipose tissue remains poorly documented and controversial'. cAMP-raising agents such as lipolytic hormones activate AMPK in adipocytes, an effect that is, at least in part, secondary to stimulation of lipolysis with the subsequent re-esterification of accumulated FAs resulting in an increase in the cellular AMP:ATP ratio [12,13]. Long-chain NEFAs also have an antilipolytic effect that may be secondary to activation of AMPK which phosphorylates hormone-sensitive lipase and decreases its activity [11,14,15]. The few studies that have addressed the potential role of AMPK as a regulator of glucose transport into adipocytes have yielded conflicting findings. In 3T3L-1 adipocytes activation of AMPK by AICAR (5-amino-4-imidazolecarboxamide-1-β-D-ribofuranoside) stimulated basal uptake of 2-DOG (2-deoxyglucose) [16] and promoted translocation to the plasma membrane of GLUT4 [17] while reducing insulin-stimulated 2-DOG uptake [16]. By contrast overexpression of a dominant negative AMPK mutant had no effect on AICAR-induced glucose transport [18]. In rodent, primary adipocytes AICAR decreased both basal and insulin-stimulated uptake of 2-DOG [19,20]. By contrast increases in both basal and insulin-stimulated glucose uptake in response to adiponectin were blocked by inhibitors of AMPK suggesting that AMPK may play a role in the stimulation of glucose uptake [21].

Data originating from this laboratory [22] can be used to show that palmitate increases glucose utilization by rat adipocytes (see Figure 1), an effect that is the direct opposite of the Randle cycle as proposed for muscle tissues. Other studies, subsequent to that of [22] have demonstrated stimulation of 2-DOG or 3-*O*-methylglucose transport into adipocytes by various long-chain NEFAs [23–27], but the mechanism initiating this NEFA effect has remained unexplained. Informed by recent advances in knowledge of the AMPK system, we have revisited this issue. Using palmitate as a representative long-chain NEFA, we found this to cause activation of adipocyte AMPK without any alteration of the cellular AMP:ATP ratio. Additionally we found that adipocyte AMPK activity can be decreased by glucose and we investigated the effect of insulin on AMPK activity in these cells.

MATERIALS AND METHODS

Isolation and incubation of adipocytes

Adipocytes were isolated in accordance with UK Home Office procedures by collagenase digestion of epididymal fat pads from male Sprague–Dawley rats (200–250 g). Adipocytes equivalent to 1/5th of one fat pad (typically $8–10 \times 10^6$ cells) were immediately incubated for 1 h in 4 ml of incubation medium consisting of Krebs–Henseleit bicarbonate buffer [pre-equilibrated with O_2/CO_2 (19:1)] containing FA-poor albumin (20 mg/ml) and other additions as indicated.

Glucose utilization by adipocytes

This was measured experimentally as the sum of the conversion of [U-^{14}C]glucose to total lipid (FA + GG) + CO_2 together with the formation of lactate + pyruvate [28] (note: FA, long-chain fatty acid synthesized *de novo* from glucose and converted into TAG; GG, the glyceroyl moiety of TAG formed from glucose). Additionally this was calculated from data in [22] using eqn (1.8), which is described

and validated in the Supplementary Online data section (at http://www.bioscirep.org/bsr/033/bsr033e007add.htm).

2-DOG transport into adipocytes

After incubation for 1 h, 0.5 μCi of [^{3}H]2-DOG was added to adipocytes to give a final concentration of 125 μM. After 10 min transport was terminated by addition of 50 μM cytochalasin B. Adipocytes were recovered by centrifugation and washed twice with incubation medium containing cytochalasin B and then solubilized in 0.1 M NaOH prior to scintillation counting. Cytochalsin B was added simultaneously with [^{3}H]2-DOG in blank assays. Since the cells were washed under conditions where sugar transport was inhibited, 2 mM sodium pyruvate was present in the incubation and washing media in order to avoid compromising the cellular energy status.

Activity assay of adipocyte α-1 AMPK

Adipocytes were recovered by brief centrifugation and lysed in 1 ml of ice-cold 50 mM Tris/HCl (pH 7.5), 1 mM EDTA, 1 mM EGTA, 50 mM NaF, 5 mM $Na_4P_2O_7$, 10 % (v/v) glycerol, 1 % (v/v) Triton X-100, 1 mM DTT (dithiothreitol), 1 mM PMSF, 1 mM benzamidine and SBTI (soya-bean trypsin inhibitor) (4 μg/ml). The lysate was centrifuged at 13 000 ***g*** for 10 min at 4 °C and aliquots of the supernatant were used for immunoprecipitation of α-1 AMPK followed by activity assay in the presence of 200 μM AMP using 200 μM SAMS peptide as a substrate [6].

Adipocyte adenine nucleotide contents

Adipocyte incubations were terminated with $HClO_4$ and ATP, ADP and AMP were measured by ion-pair RP-HPLC (reverse-phase HPLC) [29].

Adipocyte DNA contents

DNA was measured by reaction with diphenylamine using calf thymus DNA as a standard. A total of 1 g of epididymal fat pad yielded 135 ± 4 μg of adipocyte DNA ($n = 55$).

Expression of results and statistical methods

Glucose utilization, 2-DOG transport and α-1 AMPK activity are expressed as $\mu mol \cdot h^{-1} \cdot 100\ \mu g$ of DNA^{-1}, $pmol \cdot 10\ min^{-1} \cdot 100\ \mu g$ of DNA^{-1} and $pmol \cdot 30\ min^{-1} \cdot 100\ \mu g$ of DNA^{-1} respectively. Statistical significance was assessed by Student's t test for paired samples with $P < 0.05$ indicating a significant effect. Values of n indicate the numbers of independent adipocyte preparations. Error bars in Figures indicate S.E.M.

RESULTS

Palmitate increased adipocyte glucose utilization, 2-DOG transport and AMPK activity

Using data for FA, GG and (lactate + pyruvate) from [22], rates of glucose utilization at a range of palmitate concentrations were calculated using Method 1 described in the Supplementary Online data. At palmitate:albumin molar ratios that encompass and exceed NEFA physiological levels in the systemic and adipose tissue circulations this FA increased glucose utilization by cells incubated with 1 mM glucose alone or with 5 mM glucose and insulin (Figure 1a). At 5 mM glucose with insulin this could be attributed to a 'pull' effect due to palmitate increasing utilization of glucose-derived glycerol 3-phosphate for TAG synthesis. However, with 1 mM glucose alone where glucose transport should have greater control strength over glucose utilization the stimulatory effect of palmitate was at least as large. This suggested that palmitate might also stimulate glucose utilization by a 'push' mechanism, i.e. at the level of glucose transport. Figure 1(b) shows that cells from 24-h starved rats had a similar percentage response to palmitate as in cells from fed rats even though their basal rate of glucose utililization was decreased. Cells from 72-h starved rats had a further decrease in their basal rate of glucose utilization and a decreased, though still significant, stimulation of glucose utilization.

Direct measurements with adipocytes from fed rats incubated at 5 mM glucose without insulin confirmed an enhancement of glucose utilization by palmitate (Figure 2a). As shown in Figure 2(b), palmitate increased the activity of α-1 AMPK, the predominant form of AMPK in adipocytes [11,30]. Pooling all available measurements, we found that 1 mM palmitate increased glucose utilization by 92 ± 11 % ($n = 18$, $P < 0.0005$) and increased AMPK activity by 90 ± 15 % ($n = 25$, $P < 0.0005$). The activation of AMPK by 1 mM palmitate was not linked to an increase in the cellular AMP:ATP ratio (Figure 2c). In fact palmitate caused a significant 13 % decrease in that ratio. No significant alterations in the 'energy charge' or in the total adenine nucleotide content were seen with palmitate.

The uptake of 2-DOG (and its subsequent conversion into 2-DOG 6-phosphate) was measured as an index of glucose transport activity. It is customary to measure 2-DOG uptake in the absence of glucose or at a low glucose concentration to minimize the control strength of hexokinase relative to that for glucose transport. We always had some glucose present together with 2 mM pyruvate to ensure that the energy status of the cells was not compromised. At 1 mM glucose palmitate increased 2-DOG transport by 45 % (Figure 3c). As expected, an increase in glucose from 1 to 5 mM decreased the basal rate of 2-DOG transport. However, the percentage increase in 2-DOG transport due to palmitate was similar at 1 and 5 mM glucose (Figures 3c and 3d).

Palmitate (1 mM) in the presence of 2 % albumin gives a NEFA:albumin ratio of 3.3 which is similar to that with 2 mM NEFA at physiological plasma albumin concentration. This is a high value for systemic plasma where NEFA concentration rarely exceeds 2 mM. However, as discussed below, higher NEFA:albumin ratios can be observed within the adipose tissue circulation [31]. There was an important technical necessity to have a relatively high initial palmitate in the incubations. This is because adipocytes from fed rats avidly convert exogenous NEFA to stored TAG. For example, it can be calculated from data used for the study of [22] in which rates of glucose metabolism per incubation flask were similar to the present study that

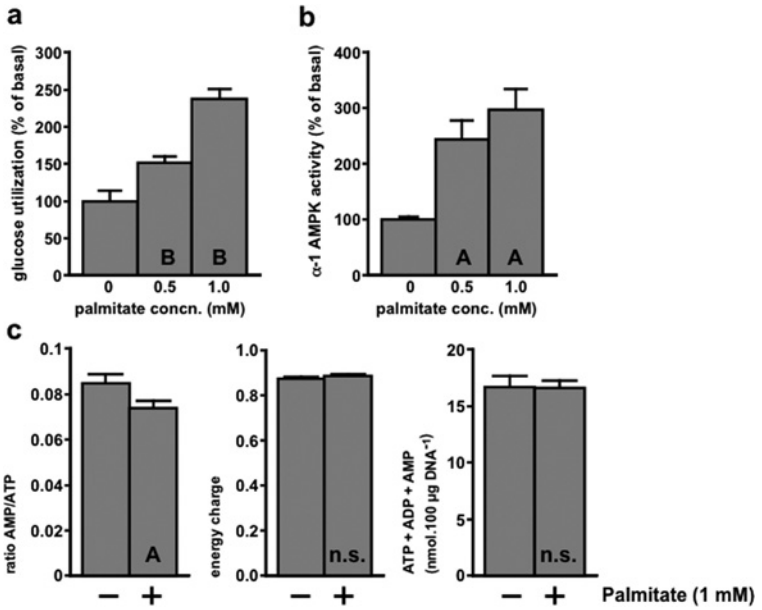

Figure 2 Palmitate increased the experimentally measured rate of net glucose utilization and α-1 AMPK activity without increasing the AMP:ATP ratio

Adipocytes were incubated for 1 h with 5 mM glucose and the indicated concentrations of sodium palmitate. n.s., A and B indicate $P > 0.05$, <0.005, <0.0005 respectively compared with the basal state without palmitate. (**a**) Conversion of [U-^{14}C]glucose into total lipid + CO_2 + (lactate + pyruvate). The basal rate of glucose utilization was 1.12 ± 0.16 μmol · h^{-1} · 100 μg of DNA^{-1} ($n = 7$). (**b**) α-1 AMPK activity. The basal activity was 16.4 ± 2.0 pmol · 30 min^{-1} · 100 μg of DNA^{-1} ($n = 6$). (**c**) Measurements of ATP + ADP + AMP. Energy charge was calculated as (ATP + 0.5×ADP)/(ATP + ADP + AMP) ($n = 15$).

adipocytes incubated for 1 h with 5 mM glucose removed 76% of available FA at 0.5 mM palmitate in the presence of 1% albumin. Insulin increased this removal to 87%. The percentage removal of FA was smaller at lower glucose concentrations or at higher albumin concentrations; e.g. at 5 mM glucose with insulin removal with 1 mM initial palmitate was 67% and 59% at 2.75% and 5% BSA, respectively. While the measurement of [U-^{14}C]glucose utilization represents the integrated activity over 1 h, measurement of 2-DOG transport is a 10 min measurement made after 1 h of incubation and AMPK measurement is just a 'snapshot' at the 1 h point. Therefore it was essential to ensure the continued presence of NEFA to the end of the incubation period if those measurements were to have any meaning. Hence, the use of 1 mM palmitate.

Compound C attenuated the enhancements of glucose utilization, 2-DOG transport and AMPK activity by palmitate

Compound C is a cell-permeable reversible ATP-competitive inhibitor of AMPK ($K_i = 109$ nM at 5 μM ATP) that substantially alters the conformation of the AMPK-activation loop [32]. It also decreases the α-Thr^{172} phosphorylation of AMPK [15] and has been shown *in vivo* to attenuate the effects of AICAR and metformin on AMPK activity [33]. Compound C abolished the enhancements of glucose utilization and AMPK activity by 1 mM palmitate (Figures 3a and 3b). In the presence of Compound C, which itself lowered the basal AMPK activity, palmitate actually caused a small but significant decrease in AMPK activity (Figure 3b). Compound C substantially lowered the basal rate of 2-DOG transport and largely decreased the enhancement of this by palmitate although a small but significant effect of palmitate was retained (Figure 3c).

Palmitate and Compound C altered the distribution of metabolic products originating from glucose (Figure 3e). Palmitate had a net 'anabolic effect', i.e. it increased the proportion of glucose converted into total lipid (FA + GG) relative to the catabolic products CO_2, lactate and pyruvate. This 'anabolic effect' was consistently seen with 11 independent cell preparations in which 1 mM palmitate increased the percentage of glucose utilization for total lipid synthesis from 51.2 ± 2.5% to 62.5 ± 2.6% ($P < 0.0005$). By contrast Compound C had a net 'catabolic effect' by decreasing the percentage of glucose utilization for total lipid synthesis ($P < 0.01$) and increasing that for CO_2 formation ($P < 0.025$), while having no effect on the percentage converted into lactate + pyruvate. Additionally Compound C abolished the 'anabolic effect' of palmitate.

The results presented in Figures 1–3 together with the published literature lead to the following conclusions. (i) At least some of the increase in glucose utilization in response to palmitate is due to a 'push' mechanism through increased glucose transport. (ii) The palmitate effect appears to be confined to

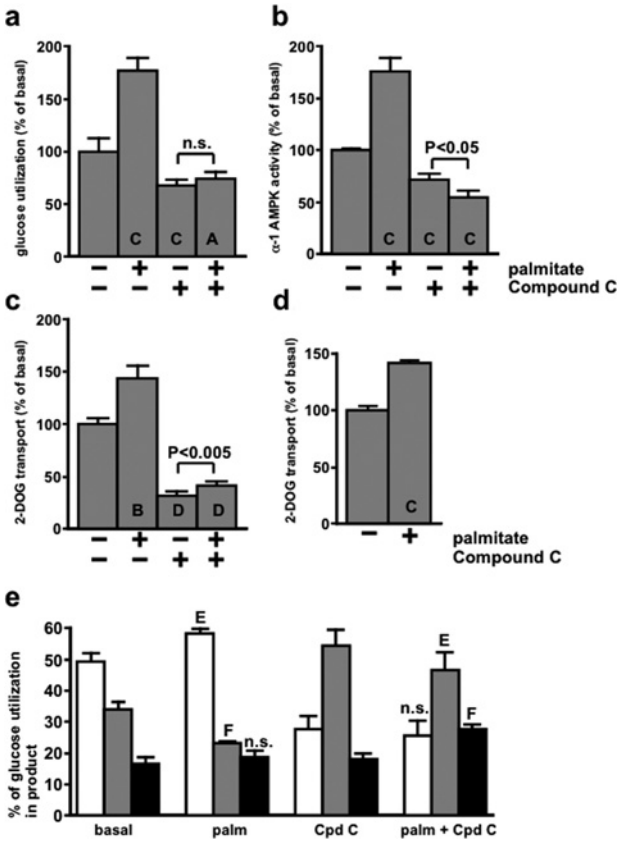

Figure 3 Compound C blocked the effect of palmitate on glucose utilization, α-1 AMPK activity and 2-DOG transport

(**a–d**) Measurements were made in adipocytes incubated for 1 h with the indicated additions of 1 mM sodium palmitate or 50 μM Compound C. n.s., A, B, C and D indicate $P > 0.05$, <0.025, <0.01, <0.005, <0.0005 respectively compared with the basal state without palmitate or Compound C. *P* values on the figures indicate the significance of the effect of palmitate in the presence of Compound C. (**a**) Conversion of 5 mM [U-^{14}C]glucose to total lipid + CO_2 + (lactate + pyruvate). The basal rate of glucose utilization was 1.27 ± 0.16 μmol · h^{-1} · 100 μg of DNA^{-1} ($n = 5$). (**b**) α-1 AMPK activity in the presence of 5 mM glucose. The basal activity was 15.9 ± 0.3 pmol · 30 min^{-1} · 100 μg of DNA^{-1} ($n = 5$). (**c**) Transport of [^{3}H] 2-DOG in the presence of 1 mM glucose. The basal rate of transport was 123 ± 7 pmol · 10 min^{-1} · 100 μg of DNA^{-1} ($n = 6$). (**d**) Transport of [^{3}H] 2-DOG in the presence of 5 mM glucose. The basal rate of transport was 30.5 ± 1.2 pmol · 10 min^{-1} · 100 μg of DNA^{-1} ($n = 9$). (**e**) The values are derived from the experiment shown in (**a**) and indicate the percentage of utilized glucose in the products total lipid (white bars), CO_2 (grey bars) and lactate + pyruvate (black bars). n.s., E and F indicate the significance of the effects of palmitate relative to the control without palmitate ($P > 0.05$, <0.025, <0.005, respectively). The significances of effects of Compound C are given in the text.

the transport/utilization of glucose and is not seen with non-glucose lipogenic precursors that enter adipocytes independently of GLUT4. For example, the utilization of fructose by adipocytes is unaffected by palmitate [28]. Most fructose transport is through GLUT5 that is entirely in the plasma membrane with no modulation of its membrane abundance by insulin [34]. Also the utilization of pyruvate that enters the cells via a monocarboxylate transporter is unaffected by palmitate [1]. (iii) The attenuation by

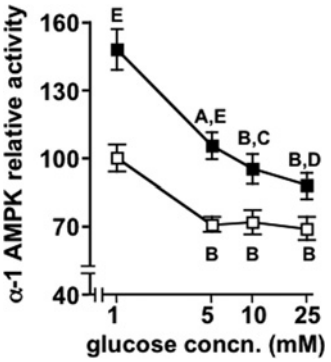

Figure 4 Glucose decreased α-1 AMPK activity

Adipocytes were incubated for 1 h with the indicated concentrations of glucose without (open symbol) or with 1 mM sodium palmitate (filled symbol). The values are expressed relative to the α-1 AMPK activity at 1 mM glucose in the absence of palmitate which was 11.7 ± 0.7 pmol · 30 min^{-1} · 100 μg of DNA^{-1} ($n = 6$). A and B indicate $P < 0.005$, <0.0005 respectively for effects of 5, 10 and 25 mM glucose versus 1 mM glucose. C–E indicate $P < 0.05$, <0.025, <0.005 for the effect of palmitate at a given glucose concentration.

Compound C of the effects of palmitate on glucose utilization, 2-DOG transport and on the palmitate 'anabolic effect' as well as its attenuation of the activation of AMPK by palmitate implies that AMPK is a mediator of these effects.

Glucose decreased adipocyte AMPK activity. Also glucose and palmitate attenuated each other's effects on AMPK activity

In the absence of palmitate increasing glucose from 1 to 5 mM decreased AMPK activity with higher glucose having no additional effect (Figure 4). Palmitate increased the concentration of glucose needed to achieve a maximal decrease in AMPK activity since the AMPK activity at 25 mM glucose was less than that at 5 mM glucose in the presence of palmitate ($P < 0.05$). Palmitate increased AMPK activity at all glucose concentrations although the percentage increase due to palmitate was less at higher glucose concentrations (49 ± 9 %, 42 ± 7 %, 22 ± 9 % and 21 ± 8 % at 1, 5, 10 and 25 mM glucose respectively). In conclusion, glucose and palmitate attenuated each other's effects on AMPK activity.

The combined effects of palmitate and insulin on glucose utilization, 2-DOG transport and AMPK activity

Insulin inactivates AMPK through an Akt [also known as PKB (protein kinase B)]-mediated phosphorylation of Ser$^{485/491}$ in the AMPK α-1/α-2 subunits [35]. Therefore we investigated combined effects of palmitate and insulin. Palmitate, insulin and (insulin + palmitate) increased 2-DOG transport relative to the basal level by 63 %, 119 % and 175 % respectively (Figure 5a). These effects showed no synergy, i.e. the combined effect was not significantly different from the sum of the individual effects ($P > 0.4$). For glucose utilization (Figure 5b) palmitate, insulin

and (insulin + palmitate) caused increases of 72 %, 162 % and 320 %. Here, the combined effect was significantly greater than the sum of the individual effects ($P < 0.005$). This synergy was not unexpected because, in addition to stimulating glucose transport, palmitate has a 'pull' effect on glucose utilization through being a co-substrate with glucose-derived glycerol 3-phosphate for TAG synthesis. An increase in glucose transport by insulin would be expected to potentiate this 'pull' effect.

Insulin had no effect on basal AMPK activity but decreased AMPK activity when palmitate was present leading to a reduction in, but not a total ablation of, the activation of AMPK by palmitate (Figure 5c). Insulin had no effect on the cellular AMP:ATP ratio (Figure 5d). Compared with the basal state insulin + palmitate in combination caused a small but significant decrease in the AMP:ATP ratio (Figure 5d) and increased the 'energy charge' from 0.887 ± 0.008 to 0.902 ± 0.004 ($n = 5$, $P < 0.005$) without any change in the total content of adenine nucleotides (results not shown). These small changes in the cellular-energy status appeared to be insufficient to alter AMPK activity (Figure 5c).

Figure 5(e) presents results from Figures 5(a)–5(c) expressed as the percentage enhancements caused by palmitate in the presence and absence of insulin. When expressed in this manner, insulin was seen to diminish the percent effectiveness of palmitate to increase 2-DOG transport. This was not unexpected because activation of AMPK appeared to mediate the effect of palmitate on 2-DOG transport (Figure 3) and insulin diminished the percent effectiveness of palmitate to increase AMPK activity (Figure 5e). The activation of AMPK by palmitate in the presence of insulin was small. That this could be attributed to excessive removal of palmitate prior to the 'snapshot' measurement of AMPK activity at 1 h is most unlikely because in the presence of insulin palmitate increased 2-DOG transport as measured after 1 h (Figure 5a). A more detailed study of the effects of several concentrations of palmitate and insulin on 2-DOG transport and AMPK activity is necessary in order to establish whether such a small activation of AMPK is sufficient to cause the activation of 2-DOG transport by palmitate in the presence of insulin. By contrast with the effect on 2-DOG transport insulin had minimal effect on the percentage stimulation of glucose utilization by palmitate. We attribute this to palmitate's additional role as a co-substrate with glucose-derived glycerol 3-phosphate in TAG synthesis (the 'pull' effect).

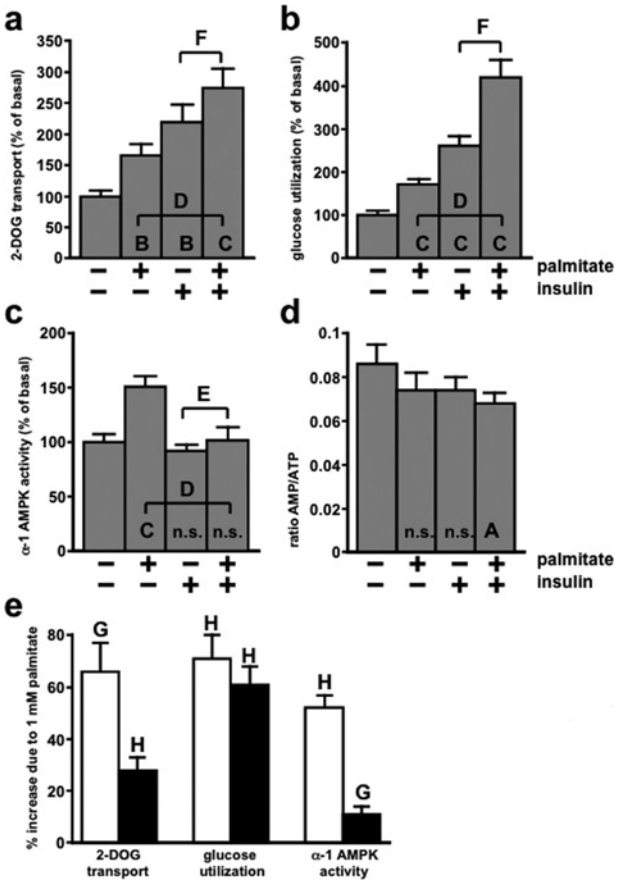

Figure 5 The effects of palmitate and insulin on glucose utilization, 2-DOG transport, α-1 AMPK activity and the cellular AMP:ATP ratio

(**a**–**d**) Measurements were made in adipocytes incubated for 1 h with the indicated additions of sodium palmitate (1 mM) or insulin (10 nM). n.s, A, B and C indicate $P > 0.05$, $P < 0.01$, <0.005, <0.0005, respectively compared with the basal state. D indicates $P < 0.0005$ for the effect of insulin in the presence of palmitate. E and F indicate $P < 0.005$, <0.0005 respectively for the effect of palmitate in the presence of insulin. (**a**) Transport of [^{3}H] 2-DOG in the presence of 1 mM glucose. The basal rate of transport was 148 ± 14 pmol · 10 min^{-1} · 100 μg of DNA^{-1} ($n = 9$). (**b**) Conversion of 5 mM [U-^{14}C]glucose into total lipid + CO_2 + (lactate + pyruvate). The basal rate of glucose utilization was 2.23 ± 0.23 μmol · h^{-1} · 100 μg of DNA^{-1} ($n = 7$). (**c**) α-1 AMPK activity in the presence of 5 mM glucose. The basal activity was 14.8 ± 1.2 pmol · 30 min^{-1} · 100 μg of DNA^{-1} ($n = 8$). (**d**) AMP:ATP ratios in the presence of 5 mM glucose. The 'energy charge' in the basal state was 0.887 ± 0.008 and with palmitate + insulin was 0.902 ± 0.004 ($P < 0.005$; $n = 5$). (**e**) The values are derived from the experiments shown in (**a**–**c**) to indicate the percentage effects of palmitate on 2-DOG transport, glucose utilization and α-1 AMPK activity in the absence (white bars) or presence (black bars) of insulin. G and H indicate $P < 0.005$ and <0.0005 respectively for effects of palmitate.

DISCUSSION

As was observed previously in heart [6] and in L6 skeletal muscle myotubes [7,8] adipocyte AMPK was increased by long-chain NEFA, e.g. palmitate, oleate and linoleate. In the present study, we have just used palmitate as a representative long-chain NEFA. While it is possible that in adipocytes this effect is specifically confined to palmitate we expect that to be unlikely in view of the previously reported effects of a wider range of FAs. In previous studies, changes in AMPK activity were correlated with increased α-Thr^{172} phosphorylation of AMPK [6–8]. We attempted to make the same correlation but in our hands satisfactory measurements of α-Thr^{172} phosphorylation were prevented by carry-over of albumin from the incubation medium into cell extracts that interfered with the Western blotting procedure. We tried to obviate this by washing the cells in albumin-free medium prior to freeze-stopping but that delay in freeze-stopping caused large

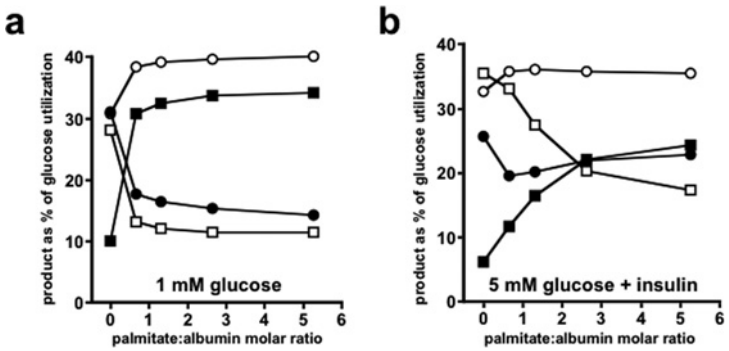

Figure 6 Effect of palmitate on the distribution of glucose-derived metabolic products in adipocytes from fed rats
Data from Table 3 of [22] were used as in Figure 1(a) to calculate glucose utilization. Eqn (1.1) in the Supplementary Online data section (at http://www.bioscirep.org/bsr/033/bsr033e007add.htm) was then used to derive values for CO_2 formation. All values were then expressed as percentages of glucose utilization. Each data point is the mean of five independent experiments. (**a**) Incubation with 1 mM glucose. (**b**) Incubation with 5 mM glucose + 0.2 μM insulin. FA: open squares; GG: filled squares; CO_2: open circles; (lactate + pyruvate): filled circles.

variations in the measurements of α-Thr^{172} phosphorylation. No significant change in total AMPK protein was observed after exposure to palmitate for 1 h (results not shown) and since the increase in AMPK activity with palmitate survived cell extraction and immunoprecipitation (procedures that would eliminate allosteric effects), we concluded that the increase in AMPK activity with palmitate must be due to covalent modification. As also was observed previously in heart and L6 skeletal muscle myotubes [6,7] the activation of adipocyte AMPK by NEFA occurred in the absence of any detectable change in the cellular AMP:ATP ratio. The mechanism of that effect is not fully understood, but a study *in vitro* has suggested that NEFA enhances the ability of the upstream AMPK LKB1 to phosphorylate AMPK α-Thr^{172} through an allosteric interaction of FA with the AMPK $\beta\gamma$-subunits [8]. An adenine nucleotide-independent activation of adipocyte AMPK in response to NEFA is contrary to the observation that lipolytic agents such as forskolin and isoprenaline increased the AMP:ATP ratio in 3T3-L1 adipocytes together with an increase in AMPK α-Thr^{172} phosphorylation [12]. Those changes were offset by orlistat and triacsin C and it was concluded that the ATP-dependent re-esterification of lipolysis-derived NEFA decreased the cellular energy state, leading to activation of AMPK. The contrast between our findings and those of [12] raises the following questions. (i) How representative of primary adipocytes are 3T3-L1 adipocytes; i.e. do those cell types differ in the response of their energy status to NEFA? (ii) Do exogenous NEFAs and those that are generated endogenously by lipolysis have different metabolic effects? As we discuss below, increases in exogenous and endogenous NEFA appear to have indistinguishable effects on glucose metabolism in primary adipocytes.

The findings in Figure 3 accord with reports that activation of AMPK by AICAR in 3T3L-1 adipocytes [16] or by adiponectin in rat adipocytes [21] led to increased transport of 2-DOG. However, our findings are at variance with observations that AICAR decreased glucose utilization by rat primary adipocytes in the absence and presence of insulin [19,20]. We offer the following explanation for this. The major anabolic products that adipocytes manufacture from glucose are FA and GG. GG esterifies newly synthesized FA and NEFA generated exogenously by LPL (lipoprotein lipase). GG also re-esterifies some lipolytic NEFA. Without the provision of some exogenous or lipolytic NEFA, the proportion of glucose utilization that is committed to FA synthesis under basal conditions normally is comparable with or higher than that committed to GG formation. Insulin increases the FA:GG ratio. However, as shown in Figure 6, provision of NEFA appreciably reverses this proportionality – an effect that can be seen over a wide range of glucose concentrations with or without insulin (Supplementary Figure S8 at http://www.bioscirep.org/bsr/033/bsr033e007add.htm). In the studies of [19,20] exogenous NEFAs were not added to the adipocyte incubations. Under those conditions potential enhancement of glucose utilization due to stimulation of glucose transport activity by AICAR/AMPK could be counteracted by a decrease in glucose utilization for FA synthesis as a result of AMPK phosphorylating and inactivating ACC. The greater the proportion of net glucose utilization for FA synthesis, the greater could be this counteractive effect. Therefore AICAR could decrease net glucose utilization, particularly when insulin is present and FA synthesis is high. However, with NEFA present stimulation of glucose transport by AICAR/AMPK would be accompanied by increased glucose utilization for GG formation and the enhancement of glucose utilization ought to predominate over a decreased percentage glucose utilization for FA synthesis with a net increase in glucose utilization being the outcome. We suggest that inactivation of ACC through its AMPK phosphorylation site is only one contributor to the rate of FA synthesis that is actually observed (rather than the percentage of glucose utilization committed to FA synthesis). Other contributing factors may be (i) increased provision of its acetyl-CoA substrate secondary to increased glucose transport and (ii) inhibition of ACC at higher NEFA concentrations – presumably due to an increased cellular level of fatty acyl-CoA. These suggestions

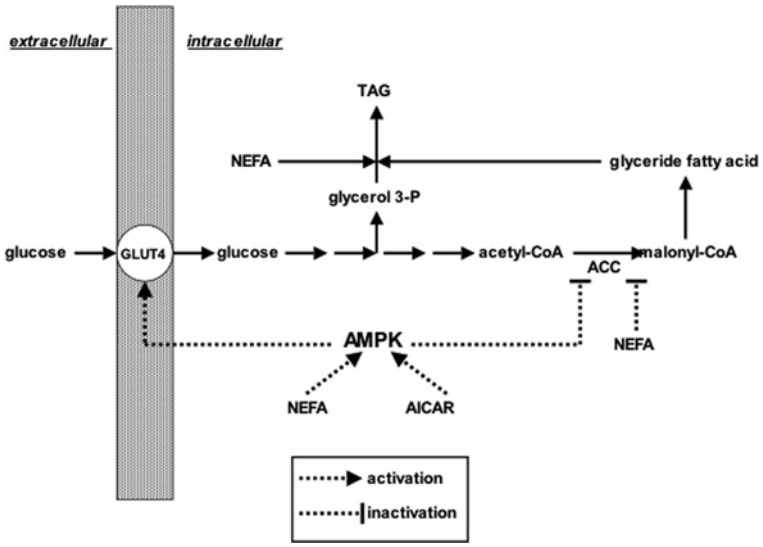

Figure 7 Scheme suggesting how the availability of NEFA could alter the metabolic fate of glucose and so alter the net effect of AICAR on glucose utilization by adipocytes

(i) Both NEFA and AICAR cause α-Thr^{172} phosphorylation and activation of AMPK. (ii) AMPK increases glucose transport by an undefined mechanism which then provides glycerol 3-phosphate for TAG synthesis and also provides the acetyl-CoA precursor for *de novo* biosynthesis of FA. However AMPK phosphorylates and inactivates ACC, thereby decreasing the potential for FA biosynthesis. (iii) Provision of NEFA results in increased generation of fatty acyl-CoA thioesters which are (a) precursors for TAG synthesis and (b) allosteric inhibitors of ACC. (iv) The net result is that at minimal NEFA availability glucose utilization for FA biosynthesis can predominate over its conversion into GG (via glycerol 3-phosphate) and activation of AMPK by AICAR would be expected to decrease net glucose utilization. However, at higher NEFA availability glucose percentage conversion to glyceride glycerol becomes more significant and its percentage use for FA biosynthesis is diminished. Under these conditions AICAR would be expected to increase net glucose utilization.

are summarized in Figure 7 and are supported by the following. With 1 mM glucose in the absence of insulin where glucose transport is likely to have appreciable control strength over glucose utilization palmitate substantially decreased the percentage of glucose committed to FA synthesis but the absolute decrease in this process was small (Supplementary Table S1a and Figure S9 at http://www.bioscirep.org/bsr/033/bsr033e007add.htm). By contrast, with 5 mM glucose and insulin, although palmitate decreased the percentage of glucose committed to FA synthesis, lower concentrations of palmitate actually increased FA synthesis (Supplementary Table S1b and Figure S9). These data are not at variance with the notion that provided there is sufficient intracellular glucose provision an enhancement of glucose transport by NEFA could generate sufficient extra acetyl-CoA to counteract the reduction of the catalytic potential of ACC due to its phosphorylation by AMPK. The decline in the increase in FA synthesis at higher concentrations of palmitate could be due to allosteric inhibition of ACC by fatty acyl-CoA. At very low glucose concentrations (i.e. 0.3 or 0.6 mM) palmitate decreased FA synthesis but at 2.5 and 5 mM FA synthesis was increased by palmitate in the absence or presence of insulin (Supplementary Table S2 at http://www.bioscirep.org/bsr/033/bsr033e007add.htm). This further illustrates how glucose provision can dictate the effect of palmitate on FA synthesis. The possible physiological significance of an activation of FA synthesis by NEFA is discussed below. Supplementary Tables S1 and S2 also demonstrate the substantial increase that palmitate brings about in increasing both the absolute rate of GG formation and the percentage contribution of glucose utilization to that process. NEFAs are as much a part of the environment of the adipocyte as glucose because these are provided in the fed state by LPL and in the fasted state by lipolysis. As far as we are aware the effect of AICAR on adipocyte glucose utilization and transport in the presence of exogenous NEFA has not been investigated. In principle AICAR and NEFAs could have additive effects since ZMP (AICAR monophosphate) derived from AICAR interacts allosterically with AMPK to decrease its propensity for dephosphorylation by protein phosphatases [36], whereas NEFAs are proposed to increase AMPK's propensity for phosphorylation by LKB1 [8].

Our conclusion that the increase in 2-DOG transport in response to palmitate was mediated by AMPK is also at variance with the study of [19] which showed that 2-DOG transport in primary adipocytes was decreased by AICAR. However, those authors measured 2-DOG transport into adipocytes preincubated for 1 h in a glucose-free medium – a procedure that ought to activate AMPK even in the absence of AICAR. In our study 2 mM pyruvate was present in the 2-DOG transport studies so that the presence of 1 mM glucose did not compromise the energy status of the cells. Those authors [19] also studied the uptake of 30 μM FA by adipocytes during a 1–5 min transport assay and found that prior exposure to AICAR for 1 h decreased FA transport. It is difficult to assess whether our findings might

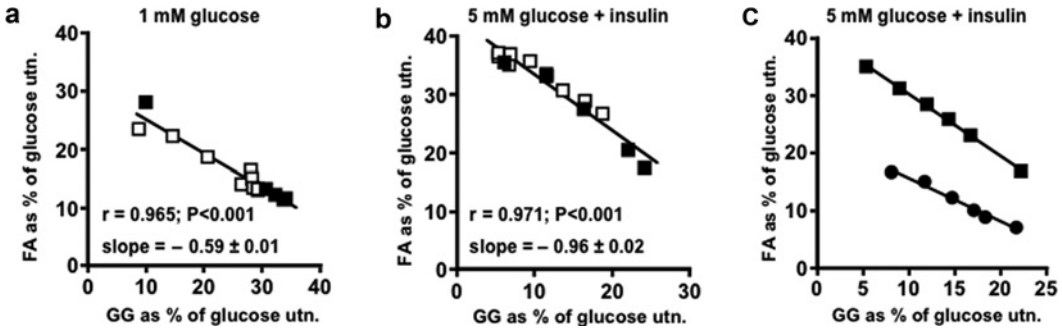

Figure 8 **The percentages of utilized glucose that are converted into FA and into GG by adipocytes are negatively correlated in a linear fashion**

(**a**, **b**) Adipocytes from fed rats were incubated for 1 h with 5% (w/v) BSA and glucose or insulin (0.2 μM) as indicated together with 0.5–4.0 mM sodium palmitate (data from Table 3 of [22]) or 0.05–5 μM adrenaline (data from Table 4 of [22]). Eqn (1.8) from the Supplementary Online data section (at http://www.bioscirep.org/bsr/033/bsr033e007add.htm) was used to calculate glucose utilization. Filled symbols: with palmitate ($n = 5$); open symbols: with adrenaline ($n = 4$). The slopes of the linear regression lines in (**a**, **b**) are significantly different ($P < 0.001$). (**c**) Data from Table 9 and Figure 3 of [22] for adipocytes incubated with 2.75% (w/v) BSA for 1 h with 5 mM glucose + insulin (0.2 μM) together with 0.25–2.0 mM sodium palmitate were used to calculate glucose utilization as in Figure 1(b). Squares: cells from fed rats. The regression line is $y = -1.072 + 0.035$ ($r = 0.999$, $P < 0.001$). Circles: cells from 24 h-starved rats. The regression line is $y = -0.752 + 0.06$ ($r = 0.991$, $P < 0.001$). The slopes of these two regression lines were significantly different ($P < 0.01$). A similar plot for cells from 72 h-starved rats is not feasible because glucose incorporation into FA was very small.

be at variance with that study because the control strength of NEFA transport over NEFA utilization for TAG synthesis was not established.

The effect of palmitate to increase the percentage of glucose utilization for GG formation while decreasing that for FA synthesis is considered further in Figure 8 which shows that these values were inversely related in a linear fashion. This was true for cells incubated with 1 mM glucose (Figure 8a) or with 5 mM glucose + insulin (Figure 8b), although the slope of the regression line was lower in the former case. A similar linear relationship was seen with cells from fasted rats but with a lower slope than for cells from fed animals (Figure 8c). The expression of the FA and GG values as percentages of net glucose utilization rather than as their absolute values is a normalization procedure that allows comparison across separate experiments of the effects of exogenous palmitate with those due to NEFA generated endogenously in response to adrenaline. The percentage plots of FA compared with GG for these two conditions were found to superimpose, implying that the origin of the NEFA was immaterial to the observed effects on glucose metabolism.

In addition to inverting the relationship between glucose conversion to FA and GG, calculations leading to Supplementary Figures S10–S13 (available at http://www.bioscirep.org/bsr/033/bsr033e007add.htm) show that palmitate had other effects on glucose metabolism. These were: (i) increased conversion of glucose carbon to TCA (trichloroacetic acid) cycle CO_2; (ii) increased net cytosolic usage of NADH with increased usage for GG formation but decreased usage for lactate and FA formation; (iii) an increase in the ratio of mitochondrial:cytosolic ATP formation that is needed to satisfy the conversion of glucose carbon into FA and GG; and (iv) a decrease in the percentage contribution of PDH (pyruvate dehydrogenase) to mitochondrial NADH formation. Supplementary Figures S10–S13 show that adrenaline had similar effects to palmitate in this regard. Supplementary Figure S14 (available at http://www.bioscirep.org/bsr/033/bsr033e007add.htm) shows a normalization that allowed comparison of the effects of palmitate and adrenaline. In all cases, data from the palmitate and the adrenaline experiments were superimposed, again indicating that the origin of the NEFA was immaterial to the resulting effects on glucose metabolism.

Activation of AMPK by NEFA in catabolic tissues such as heart and skeletal muscle has been proposed to be a feedforward mechanism which activates the β-oxidation of FAs [6,8]. The same cannot apply to white adipocytes where the rate of FA β-oxidation is so low that it is greatly exceeded by the capacity of the cells to convert NEFA into TAG [37] and where palmitate has minimal effect on the $^{14}C/^{3}H$ ratio in *de novo* synthesized FAs when adipocytes are incubated with $^{3}H_2O$ together with either [U-^{14}C]glucose or [U-^{14}C]pyruvate [22] – indicating that palmitate makes little contribution to the acetyl-CoA pool. For adipocytes, we propose that increased NEFA, through an AMPK-mediated increase in glucose transport activity that leads to increased glycerol 3-phosphate formation, causes a feedforward activation of NEFA disposal into cellular TAG (Figure 9). If that is so, 'classical' generalizations about AMPK being a driver of catabolic events and suppressor of biosynthetic processes may not be universally applicable. From the data used to calculate glucose utilization in Figure 3(a) it can be shown that Compound C decreased conversion of glucose into total lipid (FA + GG) by 78 ± 6%, to (lactate + pyruvate) by 39 ± 1% and to CO_2 by 29 ± 2%, i.e. inactivation of AMPK selectively increased glucose catabolism relative to its anabolic usage.

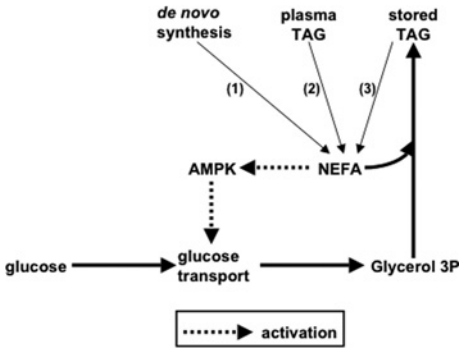

Figure 9 A hypothetical process that involves AMPK in a feed-forward activation of TAG synthesis by adipocytes

This proposes that NEFA in adipocytes derived from (1) the *de novo* synthesis of FAs, (2) from the activity of LPL or (3) from lipolytic turnover of existing stored TAG can activate AMPK. This then increases the transport into adipocytes of glucose which is a precursor for glycerol 3-phosphate, thereby facilitating the synthesis or resynthesis of stored TAG.

How an increase in glucose concentration decreases AMPK activity is unresolved. In cardiomyocytes, this may be mediated by a pentose phosphate pathway intermediate [10]. Whether the same applies to adipocytes has not been investigated.

How activation of AMPK mediates increased glucose transport activity in adipocytes is unresolved. Phosphorylation of the rab GAP (GTPase-activating protein) AS160 (TBC1D4) by the PI3K (phosphoinositide 3-kinase)/Akt pathway is necessary for the stimulation of GLUT4 exocytosis by insulin [38], but is not required for inhibition of GLUT4 endocytosis by insulin [39]. In cardiac myocytes activation of AMPK leads to increased glucose transport. This activation pathway is independent of PI3K and causes decreased endocytosis of GLUT4 without affecting GLUT4 exocytosis [3]. As shown in Supplementary Figure S15 (at http://www.bioscirep.org/bsr/033/bsr033e007add.htm) palmitate had no effect on adipocyte AS160 phosphorylation. Future studies to investigate whether palmitate decreased adipocyte GLUT4 endocytosis as a result of activation of AMPK would be interesting.

We are aware of few studies of the response of adipocyte AMPK activity to insulin. Our finding that insulin had no effect on basal AMPK activity while palmitate appeared to facilitate inactivation of AMPK by insulin was in contrast with observations that in perfused rodent hearts inactivation of AMPK by insulin occurred in the absence of NEFA but was abolished by palmitate [6,40]. Gaidhu et al. [19] found that insulin had no effect on the basal level of AMPK α-Thr^{172} phosphorylation in freshly isolated rat adipocytes, whereas the same laboratory subsequently demonstrated a decrease in basal AMPK phosphorylation in adipocytes that had been cultured for 24 h [20], suggesting that the response to insulin of adipocyte basal AMPK phosphorylation/activity may be dependent on experimental conditions (e.g. the extent of NEFA accumulation). Insulin decreased AMPK phosphorylation that had been elevated in response to forskolin in 3T3-L1 adipocytes [41] or in response to isoprenaline in rat primary adipocytes [13]. Whether those insulin effects were secondary to the antilipolytic action of insulin (thereby decreasing NEFA accumulation and subsequent AMPK activation) or were caused by NEFA directly facilitating the insulin effect on AMPK is unclear. It is noteworthy that insulin had no effect on adipocyte AMPK α-Thr^{172} phosphorylation after treatment with AICAR [19,20].

What are the physiological implications of this study? Palmitate increased adipocyte glucose utilization at palmitate:albumin ratios that are within the normal physiological range (Figure 1). However, 1 mM palmitate (palmitate:albumin = 3.3) was initially present in incubations leading to measurements of AMPK activity and we have explained the necessity to use this concentration which could be considered to be above the normal physiological range for systemic plasma. However, it is more relevant to make comparisons with NEFA concentrations in the adipose tissue circulation. Hodgetts et al. [31] have reported NEFA levels in subcutaneous adipose tissue of the human abdominal wall – a depot that appears to behave similarly to the bulk of body adipose tissue. In overnight fasted subjects at rest they observed NEFA levels in the tissue's venous drainage of 1.1 mM (NEFA:albumin = 1.72). After exercise this peaked at a median of 3.8 mM (NEFA:albumin = 5.89) with a highest recorded NEFA:albumin ratio of 7.04. Peak median values after exercise in arterialized blood from a dorsal vein draining a hand (representative of systemic plasma) were 1.85 mM (NEFA:albumin = 2.87) with a highest recorded value of 2.16 mM (NEFA:albumin = 3.35). Our use of 1 mM palmitate with 2% albumin therefore creates conditions that correspond to those seen in venous plasma in the adipose tissue circulation during exercise and it is noteworthy that Park et al. [42] found that exercise increased AMPK activity and decreased ACC activity in rat epididymal adipose tissue. The notion that increased supply of NEFAs increases glucose uptake and utilization is the direct opposite of the Randle cycle as conceived for muscle tissues. However, a fundamental feature of the Randle cycle is the β-oxidation of the increased NEFA supply [43]. We suggest that the low propensity for β-oxidation in adipocytes [37] due to (i) the very high activity of TAG synthesizing enzymes and (ii) the low activity of CPT-1 (carnitine palmitoyltransferase-1) in adipocyte mitochondria [44] could minimize any tendency for a Randle cycle-mediated decrease in glucose transport and utilization. Also, as a consequence of this low propensity for β-oxidation, adipocyte PDH could be less susceptible to inactivation in response to an increase in NEFA supply. This in turn may contribute to the ability of palmitate to increase FA synthesis – provided there is adequate glucose availability to provide the necessary acetyl-CoA. Such an increase in FA synthesis could enhance the propensity for TAG formation and deposition in adipocytes when LPL is active and is generating FAs from lipoprotein TAG in the adipose tissue capillary bed. Our study has other possible physiological implications as follows. (i) If under 'mobilizing conditions' lipolysis exceeded vascular removal of NEFA from the adipose tissue capillary bed, activation of adipocyte AMPK by NEFA could modulate NEFA release by (a) phosphorylation and inhibition of hormone-sensitive lipase

[11] and by (b) increasing glucose transport leading to NEFA re-esterification. (ii) Enhancement by NEFA of the inactivation of AMPK in response to glucose may expand the range over which AMPK activity can change during the fed/fasted transition. (iii) NEFA makes AMPK activity moderately responsive to glucose under hyperglycaemic conditions, an observation that is relative to diabetes. (iv) The production and/or release by adipocytes of adipokines such as leptin, adiponectin and visfatin is regulated by AMPK [45–49]. The present study suggests ways by which NEFA and glucose could influence cytokine production through regulation of AMPK.

AUTHOR CONTRIBUTION

Abdel Hebbachi performed the experimental work shown in Figures 2–5. The data from a previous publication [22] that were used in Figures 1, 6 and 8 together with data used for Supplementary Figures S3–S14 were from experiments performed by David Saggerson (Supplementary references as shown). David Saggerson was involved in the conception and design of the project, in the analysis and interpretation of the results and in writing the paper.

FUNDING

This work was supported by Diabetes UK [grant number 07/0003528].

REFERENCES

1 Saggerson, E. D. and Tomassi, G. (1971) The regulation of glyceride synthesis from pyruvate in isolated fat cells. The effects of palmitate and altered dietary status. Eur. J. Biochem. **23**, 109–117
2 Kurth-Kraczek, E. J, Hirshman, M. F., Goodyear, L. J. and Winder, W. W. (1999) 5′-AMP-activated protein kinase activation causes GLUT4 translocation in skeletal muscle. Diabetes **48**, 1667–1671
3 Yang, J. and Holman, G. D. (2005) Insulin and contraction stimulate exocytosis, but increased AMP-activated protein kinase activity resulting from oxidative metabolism stress slows endocytosis of GLUT4 in cardiomyocytes. J. Biol. Chem. **280**, 4070–4078
4 Kola, B., Boscaro, M., Rutter, G. A., Grossman, A. B. and Korbonits, M. (2006) Expanding role of AMPK in endocrinology. Trends Endocrinol. Metab. **17**, 205–215
5 Hutchinson, D. S., Summers, R. J. and Bengtsson, T. (2008) Regulation of AMP-activated protein kinase activity by G-protein coupled receptors: potential utility in treatment of diabetes and heart disease. Pharmacol. Ther. **119**, 291–310
6 Clark, H., Carling, D. and Saggerson, D. (2004) Covalent activation of heart AMP-activated protein kinase in response to physiological concentrations of long-chain fatty acids. Eur. J. Biochem. **271**, 2215–2224
7 Fediuc, S., Gaidhu, M. P. and Ceddia, R. B. (2006) Regulation of AMP-activated protein kinase and acetyl-CoA carboxylase phosphorylation by palmitate in skeletal muscle cells. J. Lipid Res. **47**, 412–420
8 Watt, M. J., Steinberg, G. R., Chen, Z. P., Kemp, B. E. and Febbraio, M. A. (2006) Fatty acids stimulate AMP-activated protein kinase and enhance fatty acid oxidation in L6 myotubes. J. Physiol. **574**, 139–147
9 Itani, S. I., Saha, A. K., Kurowski, T. G., Coffin, H. R., Tornheim, K. and Ruderman, N. B. (2003) Glucose autoregulates its uptake in skeletal muscle: involvement of AMP-activated protein kinase. Diabetes **52**, 1635–1640
10 Tabidi, I. and Saggerson, E. D. (2012) Inactivation of the AMP-activated protein kinase by glucose in cardiac myocytes. A role for the pentose phosphate pathway. Biosci. Rep. **32**, 229–239
11 Daval, M., Diot-Dupuy, F., Bazin, R., Hainauly, I., Viollet, B., Vaulont, S., Hajduch, E., Ferre, P. and Foufelle, F. (2005) Anti-lipolytic action of AMP-activated protein kinase in rodent adipocytes. J. Biol. Chem. **280**, 25250–25257
12 Gauthier, M. S., Miyoshi, H., Souza, S. C., Cacicedo, J. M., Saha, A. K., Greenberg, A. S. and Ruderman, N. B. (2008) AMP-activated protein kinase is activated as a consequence of lipolysis in the adipocyte: potential mechanism and physiological relevance. J. Biol. Chem. **283**, 16514–16524
13 Omar, B., Zmuda-Trzebiatowska, E., Manganiello, V., Goransson, O. and Degerman, E. (2009) Regulation of AMP-activated protein kinase by cAMP in adipocytes: roles for phosphodiesterases, protein kinase B, protein kinase A, Epac and lipolysis. Cell. Signalling **21**, 760–766
14 Sullivan, J. E., Brocklehurst, K. J., Marley, A. E., Carey, F., Carling, D. and Beri, R. K. (1993) Inhibition of lipolysis and lipogenesis in isolated rat adipocytes with AICAR, a cell-permeable activator of AMP-activated protein kinase. FEBS Lett. **353**, 33–36
15 Anthony, N. M., Gaidhu, M. P. and Ceddia, R. B. (2009) Regulation of visceral and subcutaneous lipolysis by acute AICAR-induced AMPK activation. Obesity **17**, 1312–1317
16 Salt, I. P., Connell, J. M. and Gould, G. W. (2000) 5-Aminoimidazole-4-carboxamide ribonucleoside (AICAR) inhibits insulin-stimulated glucose transport in 3T3-L1 adipocytes. Diabetes **49**, 1649–1656
17 Yamaguchi, S., Katahira, H., Ozawa, S., Nakamichi, Y., Tanaka, T., Shimoyama, T., Takahashi, K., Yoshimoto, K., Imaizumi, M. O., Nagamatsu, S. and Ishida, H. (2005) Activators of AMP-activated protein kinase enhance GLUT4 translocation and its glucose transport activity in 3T3-L1 adipocytes. Am. J. Physiol. Endocrinol. Metab. **289**, E643–E649
18 Sakoda, H., Ogihara, T., Anai, M., Fujishiro, M., Ono, H., Onishi, Y., Katagiri, H., Abe, M., Fukushima, Y., Shojima, Y. et al. (2002) Activation of AMPK is essential for AICAR-induced glucose uptake by skeletal muscle but not adipocytes. Am. J. Physiol. Endocrinol. Metab. **282**, E1239–E1244
19 Gaidhu, M. P., Fediuc, S. and Ceddia, R. B. (2006) 5-Aminoimidazole-4-carboxamide-1-β-D-ribofuranoside-induced AMP-activated protein kinase phosphorylation inhibits basal and insulin-stimulated glucose uptake, lipid synthesis and fatty acid oxidation in isolated rat adipocytes. J. Biol. Chem. **281**, 25956–25964
20 Gaidhu, M. P., Perry, R. L., Noor, F. and Ceddia, R. B. (2010) Disruption of AMPK α1 signalling prevents AICAR-induced inhibition of AS160/TBC1D4 phosphorylation and glucose uptake in primary rat adipocytes. Mol. Endocrinol. **24**, 1434–1440
21 Wu, X., Motoshima, H., Mahadev, K., Stalker, T. J., Scalia, R. and Goldstein, B. J. (2003) Involvement of AMP-activated protein kinase in glucose uptake stimulated by the globular domain of adiponectin in primary rat adipocytes. Diabetes **52**, 1355–1363
22 Saggerson, E. D. (1972) The regulation of glyceride synthesis in isolated white-fat cells. The effects of palmitate and lipolytic agents. Biochem. J. **128**, 1057–1067
23 Mukherjee, S. P., Mikherjee, C., Yeager, M. D. and Lynn, W. S. (1980) Stimulation of glucose transport and oxidation in adipocytes by fatty acids: evidence for a regulatory role in the cellular response to insulin. Biochem. Biophys. Res. Commun. **94**, 682–689
24 Joost, H. G. and Steinfelder, H. J. (1985) Insulin-like stimulation of glucose transport is isolated adipocytes by fatty acids. Biochem. Biophys. Res. Commun. **128**, 1358–1363

25 Hardy, R. W., Ladenson, J. H., Henriksen, E. J., Holloszy, J. O. and McDonald, J. M. (1991) Palmitate stimulates glucose transport in rat adipocytes by a mechanism involving translocation of the insulin sensitive glucose transporter (GLUT4). Biochem. Biophys. Res. Commun. **177**, 343–349
26 Usui, I., Haruta, T., Takata, Y., Iwata, M., Uno, T., Takano, A., Ueno, E., Ishibashi, O., Ishihara, H., Wada, H. et al. (1999) Differential effects of palmitate on glucose uptake in rat-1 fibroblasts and 3T3-L1 adipocytes. Horm. Metab. Res. **31**, 546–552
27 Murer, E., Boden, G., Gyda, M. and Deluca, F. (1992) Effects of oleate and insulin on glucose uptake, oxidation and glucose transporter proteins in rat adipocytes. Diabetes **41**, 1063–1068
28 Sooranna, S. R. and Saggerson, E. D. (1975) Studies on the role of insulin in regulation of glyceride synthesis in rat epididymal adipose tissue. Biochem. J. **150**, 441–451
29 Sellevold, O. F., Jynge, P. and Aarstad, K. (1986) High performance liquid chromatography: a rapid isocratic method for determination of creatine compounds and adenine nucleotides in myocardial tissue. J. Mol. Cell. Cardiol. **18**, 517–527
30 Lihn, A. S., Jessen, N., Pedersen, S. B., Lund, S. and Richelsen, B. (2004) AICAR stimulates adiponectin and inhibits cytokines in adipose tissue. Biochem. Biophys. Res. Commun. **316**, 853–858
31 Hodgetts, V., Coppack, S. W., Frayn, K. N. and Hockaday, T. D. R. (1991) Factors controlling fat mobilization from human subcutaneous adipose tissue during exercise. J. Appl. Physiol. **71**, 445–451
32 Handa, N., Takagi, T., Saijo, S., Kishishita, S., Takaya, D., Toyama, M., Terada, T., Shirouzu, M., Suzuki, A., Lee, S. et al. (2011) Structural basis for compound C inhibition of the human AMP-activated protein kinase α2 subunit kinase domain. Acta Crystallogr. Sect. D Biol. Crystallogr. **67**, 480–487
33 Zhou, G., Myers, R., Li, Y., Chen, Y., Shen, X., Fenyk-Melody, J., Wu, M., Ventre, J., Doebber, T., Fujii, N. et al. (2001) Role of AMP-activated protein kinase in mechanism of metformin action. J. Clin. Invest. **108**, 1167–1174
34 Hajduch, E., Darakhshan, F. and Hundal, H. S. (1998) Fructose uptake in rat adipocytes: GLUT5 expression and the effects of streptozotocin-induced diabetes. Diabetologia **41**, 821–828
35 Horman, S., Vertommen, D., Heath, R., Neumann, D., Mouton, D., Woods, A., Schlattner, U., Wallimann., U., Carling, D., Hue, L. and Rider, M. H. (2006) Insulin antagonizes ischemia-induced Thr^{172} phosphorylation of AMP-activated protein kinase α-subunits in heart via hierarchical phosphorylation of $Ser^{485/491}$. J. Biol. Chem. **281**, 5335–5540
36 Sanders, M. J., Grondin, P. O., Hegarty, B. D., Snowden, M. A. and Carling, D. (2007) Investigating the mechanism for AMP activation of the AMP-activated protein kinase cascade. Biochem. J. **403**, 139–148
37 Harper, R. D. and Saggerson, E. D. (1976) Factors affecting fatty acid oxidation in fat cells isolated from white adipose tissue. J. Lipid Res. **17**, 516–526
38 Bai, L., Wang, Y., Fan, J., Chen, Y., Qu, A., James, D. E. and Xu, T. (2007) Dissecting multiple steps of GLUT4 trafficking and identifying the sites of insulin action. Cell Metab. **5**, 47–57
39 Zeigerer, A., McBrayer, M. K. and McGraw, T. E. (2004) Insulin stimulation of GLUT4 exocytosis, but not its inhibition of endocytosis, is dependent on RabGAP AS160. Mol. Biol. Cell **15**, 4406–4415
40 Folmes, C. D., Clanachan, A. S. and Lopaschuk, G. D. (2006) Fatty acids attenuate insulin regulation of 5′-AMP-activated protein kinase and insulin cardioprotection after ischemia. Circ. Res. **99**, 61–68
41 Yin, W., Mu, J. and Birnbaum, M. J. (2003) Role of AMP-activated protein kinase in cyclic AMP-dependent lipolysis in 3T3-L1 adipocytes. J. Biol. Chem. **278**, 43074–43080
42 Park, H., Kaushik, V. K., Constant, S., Prentki, M., Przybytkowski, E., Ruderman, N. B. and Saha, A. K. (2002) Coordinate regulation of malonyl-CoA decarboxylase, *sn*-glycerol-3-phosphate acyltransferase and acetyl-CoA carboxylase by AMP-activated protein kinase in rat tissues in response to exercise. J. Biol. Chem. **277**, 32571–32577
43 Hue, L. and Taegtmeyer, H. (2009) The Randle cycle revisited: a new head for an old hat. Am. J. Physiol. Endocrinol. Metab. **297**, E578–E591
44 Saggerson, E. D. and Carpenter, C. A. (1983) The effect of malonyl-CoA on overt and latent carnitine acyltransferase activities in rat liver and adipocyte mitochondria. Biochem. J. **210**, 591–597
45 Huypens, P., Quartier, E., Pipeleers, D. and Van de Casteele, M. (2005) Metformin reduces adiponectin protein expression and release in 3T3-L1 adipocytes involving activation of AMP activated protein kinase. Eur. J. Pharmacol. **518**, 90–95
46 Giri, S., Rattan, R., Haq, E., Khan, M., Yasmin, R., Won, J. S., Key, L., Singh, A. K. and Singh, I. (2006) AICAR inhibits adipocyte differentiation in 3T3L1 and restores metabolic alterations in diet-induced obesity mice model. Nutr. Metab. **3**, 31–50
47 Fu, L., Isobe, K., Zeng, Q., Suzukawa, K., Takekoshi, K. and Kawakami, Y. (2007) β-Adrenoceptor agonists downregulate adiponectin, but upregulate adiponectin receptor 2 and tumor necrosis factor-α expression in adipocytes. Eur. J. Pharmacol. **569**, 155–162
48 Lorente-Cebrián, S., Bustos, M., Marti, A., Martinez, J. A. and Moreno-Aliaga, M. J. (2009) Eicosapentaenoic acid stimulates AMP-activated protein kinase and increases visfatin secretion in cultured murine adipocytes. Clin. Sci. **117**, 243–249
49 Lee, M. J. and Fried, S. K. (2009) Integration of hormonal and nutrient signals that regulate leptin synthesis and secretion. Am. J. Physiol. Endocrinol. Metab. **296**, E1230–E1238

Received 25 April 2012/28 August 2012; accepted 17 October 2012

Published as Immediate Publication 24 October 2012, doi 10.1042/BSR20120031

Biosci. Rep. (2013) / **33** / art:e00007 / doi 10.1042/BSR20120031

OPEN ACCESS

Original Paper

SUPPLEMENTARY DATA

Acute regulation of 5′-AMP-activated protein kinase by long-chain fatty acid, glucose and insulin in rat primary adipocytes

Abdel HEBBACHI and David SAGGERSON[1]

Institute of Structural and Molecular Biology, Division of Biosciences, University College London, Gower Street, London WC1E 6BT, U.K.

INTRODUCTION

This section provides the following. (i) Figures S1 and S2 that supplement the introduction of the paper by summarizing the major pathways of glucose and fatty acid metabolism in rat adipocytes (see these Figure legends for references [1–3]). (ii) A set of calculations of the rates of glucose-related metabolic processes in adipocytes were developed. (iii) Those calculations were applied to data from the 1972 paper of Saggerson [4] that showed the effects of a range of concentrations of palmitate and adrenaline on adipocyte glucose metabolism. This treatment allowed some further interpretations of the data of [4] that is relevant to the discussion section of the paper. It also provided the basis for comparisons of the effects of palmitate and adrenaline on adipocyte glucose metabolism.

METABOLIC FLUX CALCULATIONS

Definitions

FA, GG, L, P and TCA (trichloroacetic acid) indicate the number of μg atoms of glucose carbon converted to fatty acid, glyceride glycerol, lactate, pyruvate and TCA cycle CO_2 respectively.

Method 1: an empirical calculation of the rate of glucose utilization

Studies by [4] reported rates of conversion of glucose into FA + GG + L + P by rat adipocytes without providing any measurements of CO_2 formation. Therefore an empirical method was devised that allowed CO_2 formation to be calculated from those data thereby allowing calculation of the overall rate of glucose utilization which (see Figure S1) approximates to:

$$\text{Glucose utilization} = \text{FA} + \text{GG} + \text{L} + \text{P} + \text{CO}_2 \qquad (1.1)$$

This is where:

$$\text{CO}_2 = \text{PPP CO}_2 + \text{PDH CO}_2 + \text{TCA cycle CO}_2 \qquad (1.2)$$

To develop this method, we used the raw experimental data from studies by Saggerson and Greenbaum [5,6], who incubated pieces of rat epididymal adipose tissue and measured PPP (pentose phosphate pathway) CO_2, PDH CO_2 and TCA cycle CO_2 as well as total glucose utilization and formation of FA, GG, L and P (all expressed relative to g of wet weight of tissue). Figure S3 shows that a plot of PPP CO_2 against FA is linear with a gradient of 0.26 and an intercept of 1.83 on the PPP CO_2 axis. Therefore PPP CO_2 formation was calculated as:

$$\text{PPP CO}_2 = (0.26\text{FA}) + 1.83 \qquad (1.3)$$

A similar linear relationship between PPP CO_2 and FA can be deduced for adipocytes from the data of [7]. Also, using data for adipocytes incubated with insulin and either 2.5 or 5 mM glucose (raw data from [8] and unpublished results) a linear plot similar to Figure S3 has a gradient of 0.265 ($n = 14$, $r = 0.992$). For epididymal fat pieces or adipocytes, the formation of TCA cycle CO_2 from glucose is low unless NEFA (non-esterified fatty acids) is added to the incubations or is generated *in situ* in response to a lipolytic agent. In those instances, esterification or re-esterification of NEFA leads to a large increase in GG formation from glucose together with a large increase in TCA cycle activity to fuel the provision of the ATP for NEFA esterification and re-esterification. When a spread of values is obtained in this way Figure S4 shows that a plot of TCA cycle CO_2 against GG is linear with a gradient of 0.61 and a positive intercept of 2.92 on the GG axis. Therefore TCA cycle CO_2 formation was calculated as:

$$\text{TCA CO}_2 = 0.61\text{GG} - 2.92 \qquad (1.4)$$

On the basis that acetyl-CoA derived from glucose by adipocytes is only used for the formation of FA and TCA cycle CO_2, the μmol of PDH CO_2 is 50% of the μg atoms of carbon converted into FA and TCA cycle CO_2 and therefore:

$$\text{PDH CO}_2 = 0.5 \times (\text{FA} + 0.61\text{GG} - 2.92) \qquad (1.5)$$

[1] To whom correspondence should be addressed (email d.saggerson@ucl.ac.uk).

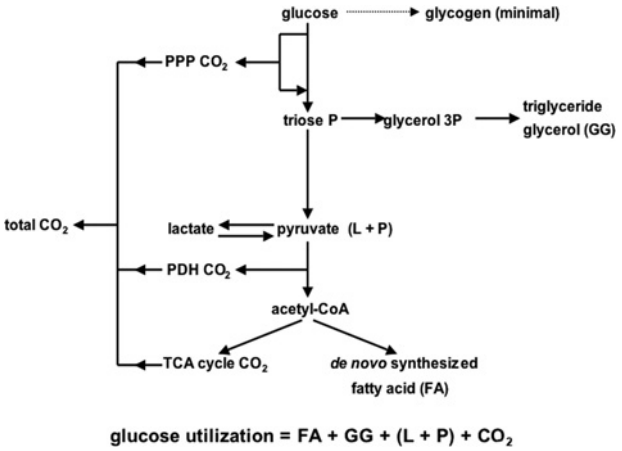

Figure S1 The adipocyte glucose economy
Based on the findings of [1] the products of glucose metabolism by rat white adipocytes can be considered to be almost entirely *de novo* synthesized FA, the glycerol moiety of TAG (GG), CO_2 (from the PPP, PDH and the TCA cycle) and accumulated lactate (L) and pyruvate (P). Synthesis of glycogen makes only a minor contribution to glucose utilization by adipocytes.

Substituting eqn (1.3), (1.4) and (1.5) into (1.2):

$$\text{Total } CO_2 = 0.76\text{FA} + 0.92\text{GG} + \text{L} + \text{P} - 2.6 \qquad (1.6)$$

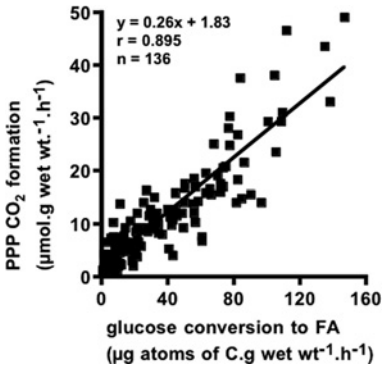

Figure S3 The relationship between glucose conversion into pentose phosphate pathway CO_2 and fatty acid formation
The data are for rat epididymal adipose tissue pieces and are taken from [5,6]. Each point is for a separate incubation.

Substituting eqn (1.6) into eqn (1.1):

$$\text{Glucose utilization} = 1.76\text{FA} + 1.92\text{GG} + \text{L} + \text{P} - 2.6 \qquad (1.7)$$

The value of $-2.6\ \mu$g atoms of C per g of wet weight is very small compared with the summation of the other values (see Figure S5) and therefore can be ignored. This reduces eqn (1.7) to eqn (1.8), which is not limited solely to use with data expressed per g of wet weight and can be used with data expressed in other

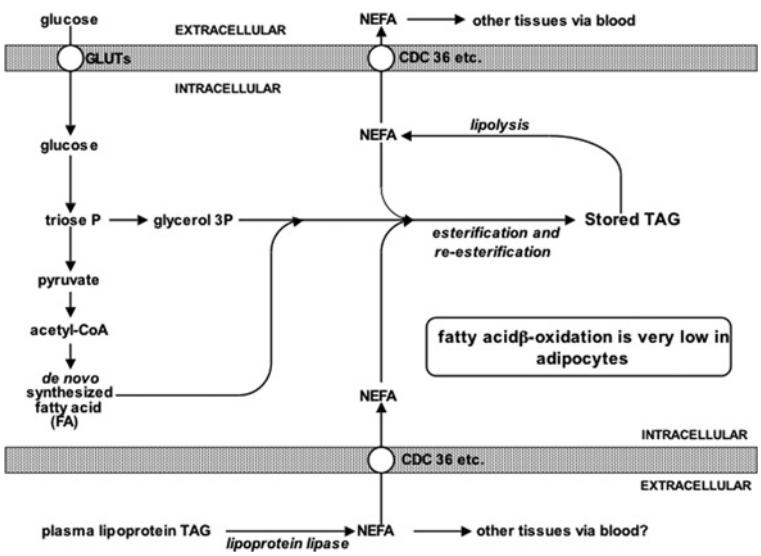

Figure S2 The adipocyte fatty acid economy
NEFAs from three sources are precursors of the rat white adipocyte's store of TAG. These NEFAs originate from: (i) the action of lipoprotein lipase in the adipose tissue capillary bed followed by transport of NEFA into the cell; (ii) intracellular *de novo* synthesis of FA; (iii) re-esterification of some of the NEFA produced in lipolysis with the remainder exiting the cell and being removed by blood flow. To provide glycerol 3-phosphate for NEFA esterification/re-esterification GLUT4 is the predominant transporter of glucose together with some contribution by GLUT1. Influx and efflux of NEFA are envisaged as predominantly being facilitated by CDC 36 and possibly by other NEFA transporters. The arrows indicate the directions of net NEFA fluxes. Under high insulin conditions (e.g. feeding) esterification and re-esterification predominate over lipolysis whereas under low insulin conditions (e.g. fasting and diabetes) lipolysis predominates. The rate of fatty acid β-oxidation makes only a very small contribution to overall NEFA metabolism in white adipocytes [2,3].

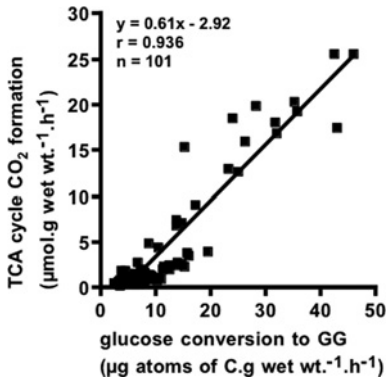

Figure S4 The relationship between glucose conversion to TCA cycle CO_2 and glyceride glycerol formation
The data are from the same experiments as in Figure S3. Each point is for a separate incubation.

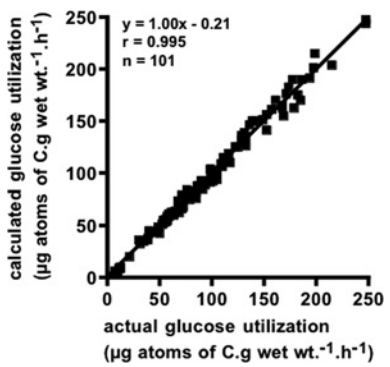

Figure S5 The correlation between calculated rates of glucose utilization and directly measured rates
The data are from the same experiments as in Figures S3 and S4. Each point is for a separate incubation. Direct measurement of glucose utilization was as for eqn (1.1). Eqn (1.8) was used to calculate glucose utilization without the use of experimental measurements of CO_2 formation.

ways (e.g. relative to DNA or protein):

$$\text{Glucose utilization} = 1.76\text{FA} + 1.92\text{GG} + \text{L} + \text{P} \qquad (1.8)$$

Equation (1.8) provides Method 1 for calculation of glucose utilization and is validated by Figure S5 that shows a linear plot of calculated glucose utilization against actual measured glucose utilization (total lipid + total CO_2 + L + P) with a gradient of 1.00 and passing very close to the graph origin. Other similar linear plots provided further validation of the method. These used data for epididymal fat pieces from [1,9] (gradient = 0.994, $n = 5$, $r = 0.989$) and from [10] (gradient = 0.999, $n = 4$, $r = 0.995$) as well as for isolated adipocytes from [7] (gradient = 0.983, $n = 5$, $r = 0.981$) and from [10] (gradient = 1.009, $n = 14$, $r = 0.995$).

Method 2: calculation of the rate of glucose utilization

This provided an alternative method for calculation of glucose utilization from the FA + GG + L + P values found in [4]. It additionally provided the basis for estimations of the contributions of various metabolic processes as shown below. The following assumptions are made. (i) ATP utilization for the conversion of glucose carbon into lipid (FA + GG) equals glucose metabolism to provide this ATP by oxidative and substrate level phosphorylations. (ii) The average chain length of FA formed from glucose carbon is C-17 (approximately 50% C-16 and 50% C-18). (iii) All of the cytosolic acetyl-CoA used for FA synthesis is formed by ATP citrate lyase. (iv) 0.26 μmol of PPP CO_2 (equivalent to 0.52 μmol of PPP NADPH) are produced per μg atom of glucose carbon incorporated into FA. (v) NADPH for FA synthesis is provided solely by the PPP or from cytosolic NADH via the concerted actions of cytosolic NAD-malate dehydrogenase and NADP-malate dehydrogenase. (vi) The reoxidation of each μmol of NADH or $FADH_2$ by the mitochondrial respiratory chain coupled to oxidative phosphorylation gives rise to 2.5 or 1.5 μmol of ATP respectively. (vii) Mitochondrial/cytosolic shuttling of reducing equivalents only involves NAD-linked redox reactions, i.e., glycerol phosphate shuttle activity is insignificant.

Values are μmol of ATP, NADH or $FADH_2$ per μg of atom of glucose C in a product.

ATP utilization for FA synthesis

(i) Hexokinase + phosphofructokinase = 0.5FA; (ii) ACC = 7.5FA/17 = 0.441FA; (iii) ATP citrate lyase = 8.5FA/17 = 0.5FA; (iv) pyruvate carboxylase = 6.16FA/17 = 0.362FA. Synthesis of 1 μmol of C-17 fatty acid requires 15 μmol of NADPH. 8.84 (0.52×17) μmol of this NADPH is provided by the PPP (see above) leaving 6.16 μmol to be provided by NADP-malate dehydrogenase. That reaction depletes oxaloacetate/malate necessitating an equivalent anaplerotic replenishment by the ATP-dependent pyruvate carboxylase reaction.

$$\text{TOTAL} = 1.803\text{FA} \qquad (2.1)$$

ATP utilization for GG formation

(i) Hexokinase + phosphofructokinase = 0.333GG; (ii) Fatty acyl-CoA synthetase = 2GG:

$$\text{TOTAL} = 2.333\text{GG} \qquad (2.2)$$

Summing eqn (2.1) and eqn (2.2), ATP utilization for FA + GG formation is:

$$1.803\text{FA} + 2.333\text{GG} \qquad (2.3)$$

ATP formation by substrate level phosphorylations

(i) Formation of accumulated lactate and pyruvate = 0.333P + 0.333L; (ii) Formation of pyruvate subsequently converted into acetyl-CoA = 0.5FA + 0.5TCA; (iii) TCA cycle

(1 GTP per 2 CO_2) = 0.5TCA:

$$\text{TOTAL} = 0.333\text{P} + 0.333\text{L} + 1.0\text{TCA} + 0.5\text{FA} \quad (2.4)$$

ATP formation by oxidative phosphorylation following reoxidation of cytosolic reducing equivalents by the respiratory chain

The following processes result in formation (F) of cytosolic NADH. (i) Glucose → accumulated pyruvate = 0.333P; (ii) Glucose → pyruvate subsequently converted into acetyl-CoA = 0.5FA + 0.5TCA. The following processes result in utilization (U) of cytosolic NADH: (iii) reduction of dihydroxyacetone phosphate to glycerol 3-phosphate = 0.333GG; (iv) The concerted actions of NAD- and NADP-malate dehyrogenases to provide NADPH for FA synthesis = 0.36FA. Formation of lactate involves no net formation of NADH and is omitted from this calculation.

Net cytosolic NADH balance (F − U) is:

$$0.333\text{P} + 0.5\text{FA} + 0.5\text{TCA} - 0.333\text{GG} - 0.36\text{FA} \quad (2.5)$$

Reoxidation of this by the respiratory chain/oxidative phosphorylation yields ATP as:

$$0.833\text{P} + 0.35\text{FA} + 1.25\text{TCA} - 0.833\text{GG} \quad (2.6)$$

ATP formation by oxidative phosphorylation following reoxidation of mitochondrial reducing equivalents by the respiratory chain

(i) The PDH NADH yield is 0.5FA + 0.5TCA which is equivalent to 1.25×(FA + TCA) ATP; (ii) the TCA cycle yields of NADH and $FADH_2$ are 1.5TCA and 0.5TCA, respectively yielding (3.75 + 0.75)TCA ATP. Therefore formation of ATP by mitochondrial processes is:

$$1.25\text{FA} + 5.75\text{TCA} \quad (2.7)$$

If ATP utilization is matched by ATP formation then eqn (2.3), eqn (2.4), eqn (2.6) and eqn (2.7) can be combined to give:

$$\begin{aligned} &1.803\text{FA} + 2.333\text{GG} \\ &= 0.333\text{P} + 0.333\text{L} + 1.0\text{TCA} + 0.5\text{FA} + 0.833\text{P} + 0.35\text{FA} \\ &\quad +1.25\text{TCA} - 0.833\text{GG} + 1.25\text{FA} + 5.75\text{TCA} \end{aligned} \quad (2.8)$$

This allows TCA CO_2 formation to be calculated as:

$$\text{TCA} = 0.396\text{GG} - 0.037\text{FA} - 0.146\text{P} - 0.041\text{L} \quad (2.9)$$

Since total CO_2 formation = PPP CO_2 + PDH CO_2 + TCA cycle CO_2 (1.2), PPP CO_2 formation = 0.26FA and PDH CO_2 = 0.5×(FA + TCA), total CO_2 formation can be calculated:

$$CO_2 = 0.70\text{FA} + 0.59\text{GG} - 0.22\text{P} - 0.06\text{L} \quad (2.10)$$

Substituting this into eqn (1.1):

$$\text{Glucose utilization} = 1.70\text{FA} + 1.59\text{GG} + 0.78\text{P} + 0.94\text{L} \quad (2.11)$$

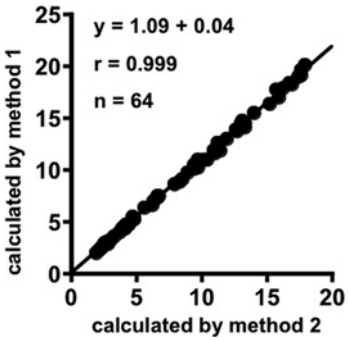

Figure S6 Comparison of Methods 1 and 2 to calculate rates of glucose utilization by rat adipocytes

Values for glucose utilization by Method 1 [eqn (1.8)] and by Method 2 [eqn (2.11)] were calculated from values for FA + GG + L + P obtained in experiments with rat adipocytes as described by [4]. Each data point is the mean of four or five independent experiments. For adipocytes from fed rats incubations contained 1 mM glucose with various concentrations of sodium palmitate, adrenaline or dibutyryl cAMP or contained 5 mM glucose and insulin (0.2 μM) with the same various concentrations of sodium palmitate, adrenaline or dibutyryl cAMP. For adipocytes from 24 h- or 72 h-fasted rats the incubations contained 5 mM glucose and insulin (0.2 μM) with various concentrations of sodium palmitate.

Eqn (2.11) provides Method 2 for calculation of glucose utilization. Although this method gave an estimate of glucose utilization that was slightly lower than that provided by Method 1 (Figure S6), these two methods were in close qualitative agreement when they were used to assess percentage effects of pamitate and adrenaline on glucose utilization (Figure S7). This provided assurance that the following expressions can reasonably be based on the Method 2 approach.

TCA cycle CO_2 formation

See eqn (2.9).

Cytosolic NADH balance (F − U)

Substituting eqn (2.9) for the TCA value in eqn (2.5) gives:

$$(\text{F} - \text{U}) = 0.26\text{P} + 0.122\text{FA} - 0.135\text{GG} - 0.02\text{L} \quad (2.12)$$

Glycolytic and mitochondrial ATP formation

ATP formation by glycolytic substrate level phosphorylation is the quantity in eqn (2.4) minus the value (0.5TCA) for TCA cycle substrate level phosphorylation, i.e.:

$$\begin{aligned} &\text{Glycolytic ATP formation} \\ &= 0.333\text{P} + 0.333\text{L} + 0.5\text{FA} + 0.5\text{TCA} \end{aligned} \quad (2.13)$$

ATP formation by mitochondrial processes is the difference between ATP utilization shown in eqn (2.3) and the glycolytic ATP formation shown in eqn (2.13).

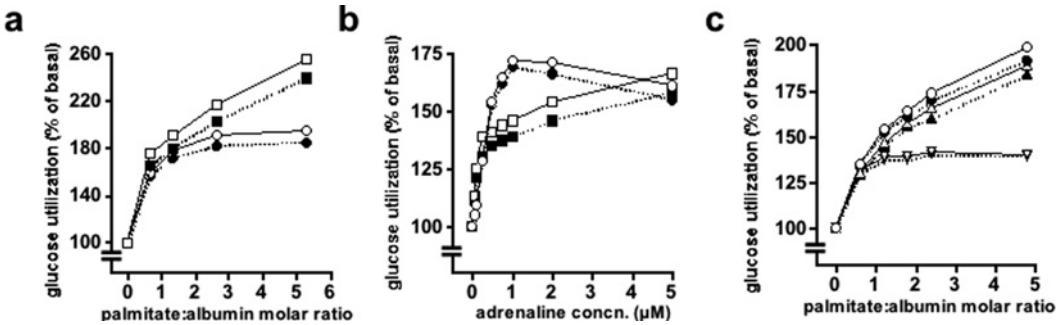

Figure S7 **Methods 1 and 2 to calculate rates of glucose utilization by rat adipocytes closely agreed when effects of palmitate, adrenaline or fasting were compared on a percentage basis**
The data are from the same experiments as in Figure S6. Open symbols: glucose utilization calculated by Method 1 [eqn (1.8)]. Filled symbols: glucose utilization calculated by Method 2 [eqn (2.11)]. Squares: 1 mM glucose, fed state. Circles: 5 mM glucose + insulin, fed state. Triangles: 5 mM glucose + insulin, 24h-fasted. Inverted triangles: 5 mM glucose + insulin, 72 h-fasted.

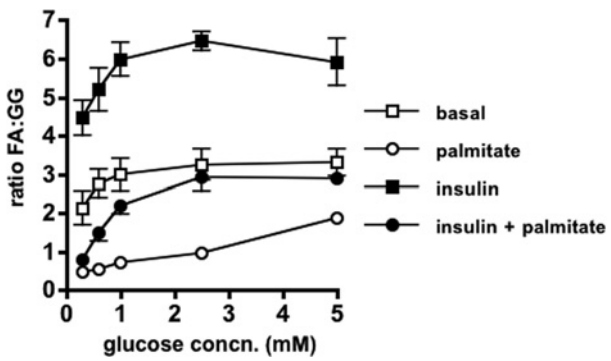

Figure S8 The effect of palmitate on the FA:GG ratio at different glucose concentrations
FA and GG values are from the original laboratory data for Figures 1 and 2 of [4]. Adipocytes ($n = 4$) were incubated for 1 h in 1% (w/v) BSA with the indicated concentrations of [U-^{14}C]glucose with or without 0.5 mM sodium palmitate or 0.2 μM insulin.

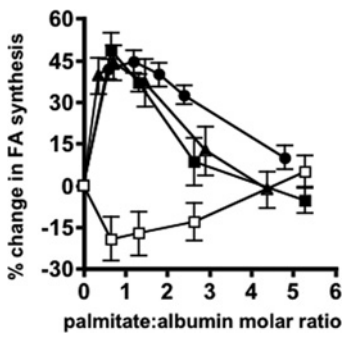

Figure S9 The effect of palmitate concentration on the conversion of glucose to fatty acids
The values are derived from the original laboratory data for the following sections of [4] in which adipocytes were incubated for 1 h either with 1 mM glucose (open symbols) or with 5 mM glucose + 0.2 μM insulin (filled symbols). Squares: from Table 3; 5% BSA; sodium palmitate from 0.5 to 4.0 mM; $n = 5$. Circles: from Figure S3; 2.75% BSA; sodium palmitate from 0.25 to 2.0 mM; $n = 5$. Triangles: from Table 7; 4.5% BSA; sodium palmitate from 0.25 to 3.0 mM; $n = 4$. Palmitate:albumin ratios are shown in order to correct for the different BSA concentrations that were used in these three experiments. In the presence of 5 mM glucose and insulin fatty acid synthesis was significantly increased at all palmitate:albumin ratios below 2.0 (P values ranging from <0.025 to <0.0005).

Mitochondrial NADH generation by PDH and the TCA cycle

$$\text{The NADH yield from PDH} = 0.5 \times (\text{FA} + \text{TCA}) \quad (2.14)$$

$$\text{The yield of NADH from the TCA cycle} = 1.5\text{TCA} \quad (2.15)$$

Therefore:

$$\text{total mitochondrial generation of NADH} = 0.5\text{FA} + 2.0\text{TCA} \quad (2.16)$$

Cytosolic usage of NADH

This is via LDH (lactate dehydrogenase), glycerol 3-phosphate dehydrogenase and via NAD-malate dehydrogenase to provide the contribution by NADP-malate dehydrogenase of NADPH for FA synthesis (see above).

$$\text{Cytosolic NADH usage} = 0.333\text{L} + 0.333\text{GG} + 0.36\text{FA} \quad (2.17)$$

RESULTS

Contents of Figures S8 and S9 and Tables S1 and S2

All of the values shown were derived from the original laboratory data of [4]. The contents of these Figures and Tables are

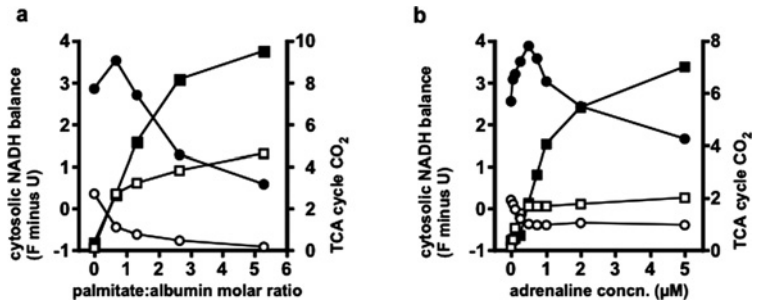

Figure S10 **The effects of palmitate and adrenaline on rat adipocyte cytosolic NADH balance and TCA cycle CO_2 formation**
The values were derived from the original laboratory data of [4] and were calculated using eqn (2.5) and eqn (2.9) for cytosolic NADH balance and TCA cycle activity, respectively. (**a**) Effects of palmitate [0.5–4 mM in the presence of 5% (w/v) BSA]. (**b**) Effects of adrenaline (0.05–5 μM). Open symbols: 1 mM glucose; filled symbols: 5 mM glucose + insulin (0.2 μM). Circles: cytosolic NADH balance (F − U) as μmol of NADH/h/100 μg cell DNA; squares: TCA cycle CO_2 as μg atoms of C/h/100 μg cell DNA.

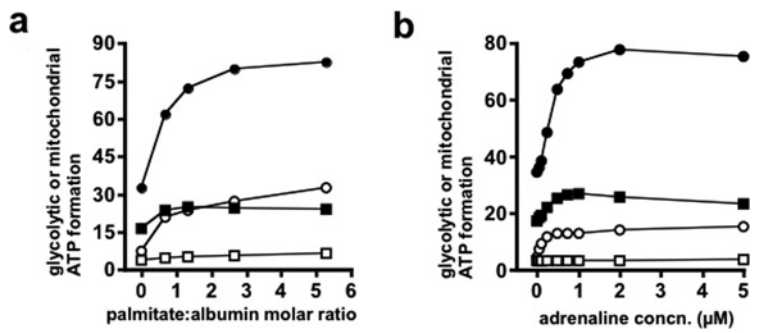

Figure S11 **The effects of palmitate and adrenaline on rat adipocyte glycolytic and mitochondrial ATP formation**
The values were calculated from the same experimental data as used for Figure S10. Glycolytic ATP formation [eqn (2.13)] was subtracted from total ATP formation [eqn (2.3)] to give mitochondrial ATP formation. (**a**) Effects of palmitate [0.5–4 mM in the presence of 5% (w/v) BSA]. (**b**) Effects of adrenaline [0.05–5 μM in the presence of 5% (w/v) BSA]. Open symbols: 1 mM glucose; filled symbols: 5 mM glucose + insulin (0.2 μM). Squares: glycolytic ATP formation; circles: mitochondrial ATP formation. Values are μmol of ATP/h/100 μg cell DNA.

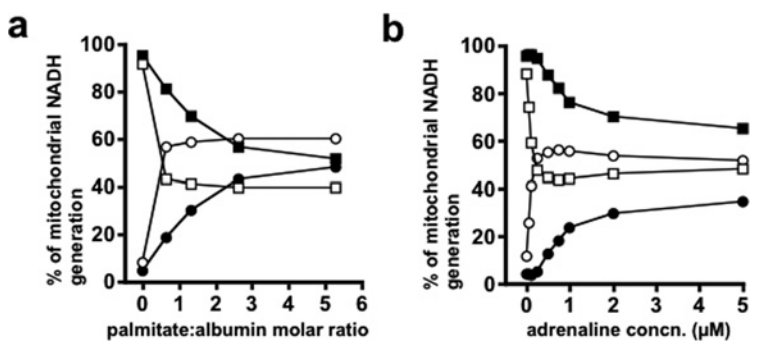

Figure S12 **The effects of palmitate and adrenaline on the proportions of mitochondrial NADH that are generated by PDH and the TCA cycle in rat adipocytes**
The values were calculated from the same experimental data as used for Figure S10. The NADH yields from PDH [eqn (2.14)] and the TCA cycle [eqn (2.15)] are expressed as percentages of the total mitochondrial generation of NADH [eqn (2.16)]. (**a**) Effects of palmitate [0.5–4 mM in the presence of 5% (w/v) BSA]. (**b**) Effects of adrenaline [0.05–5 μM in the presence of 5% (w/v) BSA]. Open symbols: 1 mM glucose; filled symbols: 5 mM glucose + insulin (0.2 μM). Squares: PDH; circles: TCA cycle.

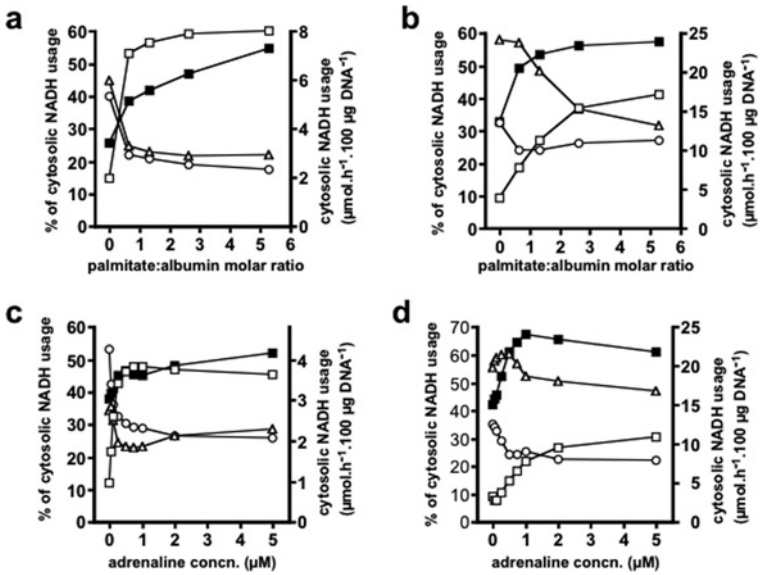

Figure S13 **The effects of palmitate and adrenaline on the usage of cytosolic NADH for the formation of GG, FA and lactate in rat adipocytes**

The values were calculated from the same experimental data as used for Figure S10. Cytosolic NADH usage was calculated by eqn (2.17) together with the percentages of this due to formation of GG, FA or lactate. Effects of palmitate (0.5–4 mM) or of adrenaline (0.05–5 μM) both in the presence of 5% (w/v) BSA are shown in (**a**,**b**) and (**c**,**d**) respectively. Filled squares: total cytosolic NADH usage. Open symbols: squares, triangles and circles for the percentage of NADH usage for formation of GG, FA and lactate respectively.

discussed in the main text. Comparison between the present study and the previous study of [4] was judged to be appropriate for the following reasons. Both studies used rats from the same animal colony, used the same procedure for adipocyte isolation and used similar conditions of incubation (bath shaking speed and 1 h of incubation). In the present study addition of 1 mM palmitate (palmitate:albumin ratio = 3.3) increased 5 mM glucose conversion into total lipid (FA + GG) by 124 ± 21% ($n = 18$) and by 89 ± 15% ($n = 7$) in the absence and presence of insulin respectively, whereas pooled data from three different experiments of [4] showed that addition of palmitate to a palmitate:albumin ratio of 2.4 ($n = 5$), 2.6 ($n = 4$) or 3.3 ($n = 4$) increased 5 mM glucose conversion into total lipid by 198 ± 24% ($n = 4$) without insulin and by 92 ± 7% ($n = 13$) with insulin. Increases in conversion of 5 mM glucose into total lipid due to addition of insulin were: this study, 164 ± 18% ($n = 7$); study of [4], 171 ± 25% ($n = 8$). We also compared percentage changes in net glucose utilization, either measured directly in the present study or from [4] as calculated from FA, GG and (lactate + pyruvate) data by Method 1 [eqn (1.8)]. Increases in 5 mM glucose utilization due to addition of palmitate in the presence of insulin were: this study, 60 ± 8% ($n = 7$); study of [4], 82 ± 4% ($n = 9$). Increases in 5 mM glucose utilization due to the addition of insulin in the absence of palmitate were: this study, 162 ± 21% ($n = 7$); study of [4], 117 ± 21% ($n = 6$). We also noted that glucose metabolism per incubation flask was similar between the studies under similar experimental conditions.

Metabolic relationships in adipocyte glucose metabolism based on the Method 2 equations

These are presented in Figures S10–S14. All values are calculated from Tables 3 and 4 of [4] which described experiments where rat adipocytes were incubated for 1 h with 5% (w/v) BSA and additions of [U-^{14}C]glucose (either 1 mM alone or 5 mM + insulin), sodium palmitate or adrenaline as indicated in the figure legends. Each data point is the mean of five and four independent experiments with palmitate and adrenaline respectively.

Figure S10 demonstrates the following. (i) Both palmitate and adrenaline substantially increased metabolism of glucose-derived carbon through the TCA cycle. (ii) At 1 mM glucose in the absence of palmitate or adrenaline the cytosolic production of NADH slightly exceeded its utilization giving a small positive (F − U) value. Both palmitate and adrenaline drove (F − U) towards a negative value, i.e. net transfer of reducing equivalents from mitochondria to cytosol would have to occur. (iii) With 5 mM glucose + insulin the (F − U) value was always positive, i.e. net transfer of reducing equivalents from cytosol to mitochondria would occur. Both palmitate and adrenaline caused an increase in the (F − U) value at low concentrations and a decrease at higher concentrations.

Figure S11 demonstrates the following. (i) Both palmitate and adrenaline substantially increased ATP formation; particularly by mitochondrial processes. (ii) Cells incubated with 5 mM glucose and insulin had a greater capacity to provide this extra ATP from glycolysis than did cells incubated with 1 mM glucose.

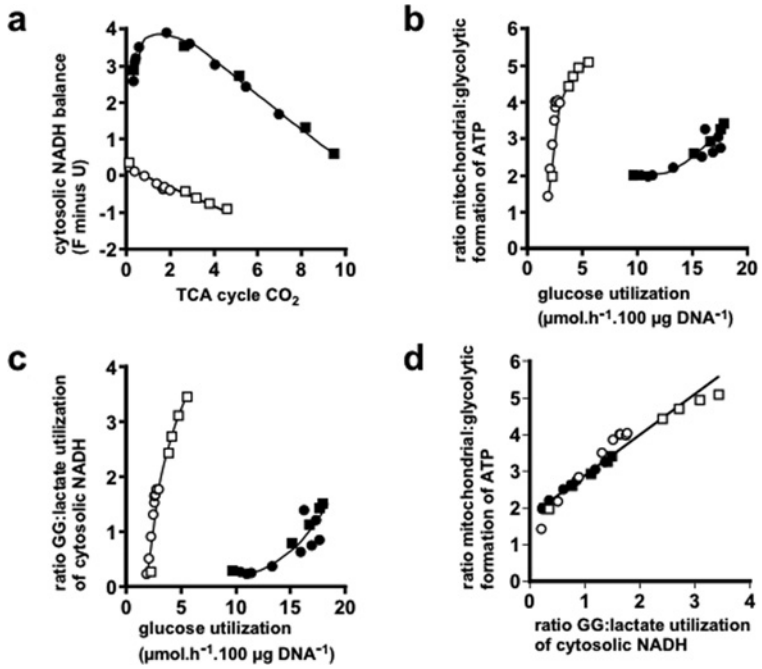

Figure S14 **Similarities between palmitate and adrenaline in their effects on the metabolism of glucose in rat adipocytes**
Open symbols: 1 mM glucose; filled symbols: 5 mM glucose + insulin (0.2 μM); squares, palmitate; closed circles, adrenaline. (**a**) Values for TCA cycle CO_2 and (F − U) are from Figures S10(a) and S10(b). A linear regression line ($y = -0.25x + 0.21$; $r = -0.962$; $P < 0.001$) is drawn through the 1 mM glucose data points and an arbitrary line is drawn through the 5 mM glucose data points. (**b**) Values for the ratio mitochondrial:glycolytic ATP formation were calculated from the data in Figures S13(a) and S13(b). Glucose utilization was calculated by eqn (2.11) from the FA, GG, L and *P* values in Tables 3 and 4 of [4]. The lines drawn through the data points are arbitrary ones. (**c**) Values for cytosolic NADH usage are from Figures S11(a)–S11(d). Glucose utilization was calculated as in (**b**). The lines drawn through the data points are arbitrary ones. (**d**) The ratios are taken from (**b**) and (**c**). A linear regression line ($y = 1.11x + 1.76$; $r = 0.972$; $P < 0.001$) is drawn through the data points.

Figure S12 shows that both palmitate and adrenaline decreased the generation of NADH by PDH while increasing TCA cycle NADH generation. Steeper concentration dependencies of these effects were seen with 1 mM glucose than with 5 mM glucose + insulin.

The reduction of dihydroxyacetone phosphate to glycerol 3-phosphate that is used in the formation of GG requires cytosolic NADH. Figure S13 shows that the total utilization of cytosolic NADH was increased by both palmitate and adrenaline and that the increased usage of NADH for GG formation was accompanied by decreased usage for lactate formation and, indirectly, for FA synthesis. At 1 mM glucose the concentration dependences of cytosolic NADH usages for lactate and FA formation were very similar in response to palmitate (Figure S13a) and in response to adrenaline (Figure S13c). By contrast, at 5 mM glucose with insulin decreased usage of cytosolic NADH for lactate formation was seen at lower concentrations of palmitate or adrenaline than were needed to cause a decrease in NADH usage for FA synthesis (Figures S13b and S13d). The observation in Figure S10 that palmitate and adrenaline cause the cytosolic NADH balance (F − U) to become negative at 1 mM glucose but not at 5 mM glucose with insulin is relevant in this regard. Presumably at 1 mM glucose cytosolic NADH is in shorter supply and has partially to be provided by transfer of reducing equivalents from mitochondria to the cytosol.

The provision of exogenous palmitate to adipocytes mimics the 'natural' routes of NEFA delivery to the cells; namely from exogenous sources via lipoprotein lipase and from endogenous TAG stores via lipolysis. In the discussion section of the paper, we consider the question of whether endogenous and exogenous NEFA would have identical metabolic effects. In consideration of this question we made the arbitrary plots shown in Figure S14. These allowed data from experiments with palmitate and adrenaline to be normalized to each other in various ways. In all four plots the data for the palmitate and the adrenaline experiments closely superimposed upon each other. In three instances (Figures S14a–S14c) the profiles with 1 mM glucose were very distinct from those with 5 mM glucose + insulin but in Figure S14(d) all of the data appeared to fall on the same curve. We suggest that this normalization approach supports the notion that the effects upon glucose metabolism of exogenous and endogenous NEFA cannot be distinguished from each other. Figure S14(b), besides according with the observation that palmitate and adrenaline increased adipocyte ATP formation/utilization (Figure S11), also

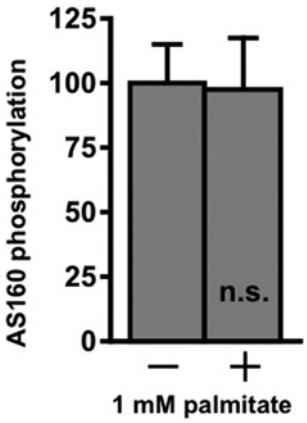

Figure S15 Palmitate did not alter the phosphorylation of adipocyte AS160

Proteins in cell lysates used for AMPK activity measurements were separated by SDS/PAGE in 4–20% Bis-Tris gels and then transferred to PVDF membranes. These were probed with phospho-(Ser/Thr) Akt substrate antibody [PAS (periodate–Schiff) antibody] followed by detection by chemiluminescence using horseradish-conjugated secondary antinody. The blots were then stripped at 50°C for 30 min in 62.5 mM Tris/HCl buffer (pH 6.8) containing mercaptoethanol (0.8%, w/v) and SDS (2%, w/v, followed by re-probing with primary antibody against total AS160 protein. Primary and secondary antibodies (from Cell Signaling Technology) were used at a 1:1000 dilution in 20 mM Tris/HCl buffer (pH 7.6) containing 137 mM NaCl, BSA (50 mg/ml) and Tween-20 (0.1%, v/v). Phospho-AS160 measurements were normalized against measurements of total AS160 protein and then expressed as percentages of the values in the absence of palmitate. n.s. indicates $P > 0.05$ for the effect of palmitate ($n = 4$).

particularly accentuated the fact that at 1 mM glucose glycolytic ATP was not able to make much contribution to the extra ATP presumably because of the diversion of much of the increased entry of glucose to GG formation. This supports the supposition in the introduction to the paper that glucose transport at 1 mM glucose availability has greater control strength over glucose metabolism than at 5 mM glucose with insulin also present.

Table S1 The effects of palmitate at fixed glucose concentrations on the conversion of glucose into FA and GG (glyceride glycerol)

Values for FA and GG are from the original laboratory data for Table 3 of [4] and are for five independent adipocyte preparations from fed rats. Glucose utilization was calculated by Method 1 [eqn (1.8)]. Adipocytes were incubated for 1 h with 5% BSA and the indicated concentrations of sodium palmitate. *Conversion rates and differences due to palmitate are expressed as μg atoms of glucose carbon $\cdot h^{-1} \cdot 100$ μg of cell DNA^{-1}.

(**a**) 1 mM [U-^{14}C]glucose without insulin

	Glucose conversion into					
	FA			**GG**		
Palmitate concentration (mM)	**Conversion rate* and percentage of glucose utilization**	**Difference***	**% Change**	**Conversion rate* and percentage of glucose utilization**	**Difference***	**% Change**
0	4.28 ± 1.40, 26.5 ± 3.6%	0	0	1.54 ± 0.26, 10.5 ± 1.0%	0	0
0.5	3.51 ± 1.46, 11.6 ± 2.8%	− 0.77 ± 0.12, $P < 0.005$	− 18	8.20 ± 1.24, 32.0 ± 2.2%	6.66 ± 1.00, $P < 0.005$	432
1.0	3.54 ± 1.53, 10.5 ± 2.8%	− 0.74 ± 0.18, $P < 0.025$	− 17	9.46 ± 1.44, 33.1 ± 1.8%	7.92 ± 1.21, $P < 0.005$	514
2.0	3.74 ± 1.55, 10.0 ± 2.5%	− 0.54 ± 0.17, $P < 0.05$	− 13	11.1 ± 1.50, 34.6 ± 2.0%	9.57 ± 1.29, $P < 0.005$	621
4.0	4.48 ± 1.86, 10.2 ± 2.4%	0.20 ± 0.48, N.S.	5	13.3 ± 1.90, 35.2 ± 2.1%	11.7 ± 1.70, $P < 0.005$	762

(**b**) 5 mM [U-^{14}C]glucose with insulin (0.2 μM)

	Glucose conversion into					
	FA			**GG**		
Palmitate concentration (mM)	**Conversion rate* and percentage of glucose utilization**	**Difference***	**% Change**	**Conversion rate* and percentage of glucose utilization**	**Difference***	**% Change**
0	22.0 ± 2.2, 35.4 ± 1.5%	0	0	3.82 ± 0.58, 6.1 ± 0.7%	0	0
0.5	32.6 ± 3.5, 32.9 ± 1.2%	10.6 ± 1.8, $P < 0.005$	48	11.5 ± 1.0, 11.8 ± 1.2%	7.7 ± 0.7, $P < 0.005$	202
1.0	30.2 ± 3.3, 27.2 ± 1.1%	8.2 ± 1.3, $P < 0.005$	37	18.2 ± 1.8, 16.7 ± 1.6%	14.4 ± 1.5, $P < 0.005$	377
2.0	24.0 ± 3.4, 20.0 ± 1.3%	2.0 ± 1.1, N.S.	9	26.1 ± 2.6, 22.4 ± 2.5%	22.3 ± 2.2, $P < 0.005$	584
4.0	21.0 ± 2.6, 17.1 ± 0.8%	− 1.0 ± 1.3, N.S.	− 5	29.5 ± 3.0, 24.5 ± 2.2%	25.7 ± 2.5, $P < 0.005$	673

Table S2 Effects of a fixed concentration of palmitate on glucose conversion into FA and GG at different glucose concentrations

Values for FA and GG are from the original laboratory data for Figures 1 and 2 of [4] and are for four independent adipocyte preparations from fed rats. Adipocytes were incubated for 1 h with 1.0% BSA and the indicated concentrations of [U-^{14}C]glucose with or without 0.5 mM sodium palmitate. *Conversion rates and differences due to palmitate are expressed as μg atoms of glucose carbon $\cdot h^{-1} \cdot 100$ μg of cell DNA^{-1}.

(**a**) Without insulin

	Glucose conversion into							
	FA				GG			
	Conversion rate*				Conversion rate*			
Glucose concentration (mM)	'Basal'	+ Palmitate	Difference*	% Change	'Basal'	+ Palmitate	Difference*	% Change
0.3	1.07 ± 0.13	0.85 ± 0.08	− 0.22 ± 0.05, $P < 0.025$	− 21	0.55 ± 0.08	1.82 ± 0.15	1.27 ± 0.11, $P < 0.005$	230
0.6	2.27 ± 0.23	1.48 ± 0.37	− 0.79 ± 0.22, $P < 0.025$	− 35	0.86 ± 0.09	3.18 ± 0.24	2.32 ± 0.16, $P < 0.0005$	270
1.0	3.23 ± 0.39	3.03 ± 0.31	− 0.20 ± 0.09, N.S.	− 6	1.11 ± 0.09	4.25 ± 0.32	3.14 ± 0.27, $P < 0.005$	283
2.5	4.73 ± 0.49	5.71 ± 0.40	0.98 ± 0.11, $P < 0.005$	21	1.47 ± 0.08	5.94 ± 0.37	4.47 ± 0.29, $P < 0.0005$	304
5.0	6.21 ± 0.53	15.3 ± 0.7	9.10 ± 0.79, $P < 0.005$	146	1.91 ± 0.12	8.49 ± 0.92	6.58 ± 0.79, $P < 0.005$	345

(**b**) With insulin (0.2 μM)

	Glucose conversion into							
	FA				GG			
	Conversion rate*				Conversion rate*			
Glucose concentration (mM)	'Basal'	+ Palmitate	Difference*	% Change	'Basal'	+ Palmitate	Difference*	% Change
0.3	5.21 ± 0.19	3.26 ± 0.37	− 1.95 ± 0.17, $P < 0.005$	− 37	1.20 ± 0.08	4.24 ± 0.19	3.04 ± 0.11, $P < 0.0005$	253
0.6	10.7 ± 0.3	9.22 ± 0.70	− 1.48 ± 0.37, $P < 0.025$	− 14	2.11 ± 0.17	6.47 ± 0.62	4.36 ± 0.46, $P < 0.005$	207
1.0	15.7 ± 0.7	17.4 ± 0.8	1.7 ± 0.8, N.S.	11	2.66 ± 0.22	8.12 ± 0.44	5.46 ± 0.27, $P < 0.0005$	205
2.5	21.1 ± 0.7	25.1 ± 1.6	4.0 ± 1.3, $P < 0.025$	19	3.29 ± 0.20	9.50 ± 0.48	6.21 ± 0.47, $P < 0.0005$	189
5.0	20.9 ± 1.2	29.6 ± 0.7	8.7 ± 0.6, $P < 0.0005$	42	3.65 ± 0.41	10.3 ± 0.4	6.67 ± 0.24, $P < 0.0005$	183

REFERENCES

1 Flatt, J. P. and Ball, E. G. (1964) Studies on the metabolism of adipose tissue. An evaluation of the major pathways of glucose catabolism as influenced by insulin and epinephrine. J. Biol. Chem. **239**, 675–685
2 Harper, R. D. and Saggerson, E. D. (1975) Some aspects of fatty acid oxidation in isolated fat cell mitochondria from rat. Biochem. J. **152**, 485–494
3 Harper, R. D. and Saggerson, E. D. (1976) Factors affecting fatty acid oxidation in fat cells isolated from white adipose tissue. J. Lipid Res. **17**, 516–526
4 Saggerson, E. D. (1972) The regulation of glyceride synthesis in isolated white-fat cells. The effects of palmitate and lipolytic agents. Biochem. J. **128**, 1057–1067
5 Saggerson, E. D. and Greenbaum, A. L. (1970) The regulation of triglyceride synthesis and fatty acid synthesis in rat epididymal adipose tissue. Biochem. J. **119**, 193–219
6 Saggerson, E. D. and Greenbaum, A. L. (1970) The regulation of triglyceride synthesis and fatty acid synthesis in rat epididymal adipose tissue. Effects of altered dietary and hormonal conditions. Biochem. J. **119**, 221–242
7 Kather, H., Rivera, M. and Brand, K. (1972) Interrelationship and control of glucose metabolism and lipogenesis in isolated fat-cells. Effect of the amount of glucose uptake on the rates of the pentose phosphate cycle and of fatty acid synthesis. Biochem. J. **128**, 1089–1096
8 Saggerson, E. D. (1974) Lipogenesis in rat and guinea-pig isolated epididymal fat-cells. Biochem. J. **140**, 211–224
9 Flatt, J. P. and Ball, E. G. (1966) Studies on the metabolism of adipose tissue. An evaluation of the major pathways of glucose catabolism as influenced by acetate in the presence of insulin. J. Biol. Chem. **241**, 2862–2869
10 Katz, J., Landau, B. R. and Bartsch, G. E. (1966) The pentose cycle, triose phosphate isomerization, and lipogenesis in rat adipose tissue. J. Biol. Chem. **241**, 727–740

Received 25 April 2012/28 August 2012; accepted 17 October 2012

Published as Immediate Publication 24 October 2012, doi 10.1042/BSR20120031